

December-2020
MEPHOJ-Vol 2 / Issue 2

MERSİN PHOTOGRAMETRY JOURNAL



EDITOR IN CHIEF

Prof. Dr. Murat YAKAR
Mersin University, Engineering Faculty
Turkey

CO-EDITORS

Assist. Prof. Dr. Ali ULVI
Mersin University, Engineering Faculty
Turkey

Assist. Prof. Dr. Osman ORHAN
Mersin University, Engineering Faculty
Turkey

ADVISORY BOARD

Prof. Dr. Orhan ALTAN
Honorary Member of ISPRS, ICSU EB Member
Turkey

Prof. Dr. Naser El SHAMY
The University of Calgary Department of Geomatics Engineering,
Canada

Prof. Dr. Armin GRUEN
ETH Zurich University
Switzerland

Prof. Dr. Ferruh YILDIZ
Konya Technical University
Faculty of Engineering and Natural Sciences
Turkey

EDITORIAL BOARD

Prof. Dr. Alper YILMAZ
Environmental and Geodetic Engineering, The Ohio State University,
USA

Prof. Dr. Dieter FRITSCH
University of Stuttgart Institute for Photogrammetry
Germany

Prof. Dr. Petros PATIAS
The Aristotle University of Thessaloniki, Faculty of Rural & Surveying Engineering
Greece

Prof. Dr. Pierre GRUSSENMEYER
National Institute of Applied Science, Department of civil engineering and surveying
France

Prof. Dr. Xiaoli DING
The Hong Kong Polytechnic University, Faculty of Construction and Environment
Hong Kong

Dr. Hsiu-Wen CHANG
National Cheng Kung University, Department of Geomatics
Taiwan

Prof. Dr. Rey-Jer YOU
National Cheng Kung University, Tainan · Department of Geomatics,
China

Prof. Dr. Bülent BAYRAM
Yıldız Technical University Engineering Faculty,
Turkey

Prof. Dr. İbrahim YILMAZ
Afyon Kocatepe University Engineering Faculty,
Turkey

Prof. Dr. Ömer MUTLUOĞLU
Konya Technical University
Faculty of Engineering and Natural Sciences,
Turkey

Dr. Öğr. Üyesi, Nizar POLAT
Harran University, Engineering Faculty,
Turkey

Dr. Öğr. Üyesi, Sefa BİLGİLİOĞLU
Aksaray University, Engineering Faculty,
Turkey

The MERSİN PHOTOGRAMMETRY JOURNAL (MEPHOJ)

THE MERSİN PHOTOGRAMMETRY JOURNAL (MEPHOJ) publishes original and innovative contributions in photogrammetric applications ranging from the integration of instruments, methodologies, and technologies and their respective uses in the environmental sciences, engineering, and other natural sciences. Mersin Photogrammetry Journal is a branch of science that widely applied in many scientific disciplines. MEPHOJ aims to cover the entirety of Photogrammetry and Photogrammetric applications about Geosciences, including their application domains. MEPHOJ strives to encourage scientists to publish experimental, theoretical, and computational results as detailed as possible so that results can be easily reproduced.

MEPHOJ is a double peer-reviewed (blind) OPEN ACCESS JOURNAL that publishes professional level research articles and subject reviews exclusively in English. It allows authors to submit articles online and track his or her progress via its web interface. All manuscripts will undergo a refereeing process; acceptance for publication is based on at least two positive reviews. The journal publishes research and review papers, professional communication, and technical notes. MEPHOJ does not charge for any article submissions or for processing.

CORRESPONDENCE ADDRESS
Journal Contact: myakar@mersin.edu.tr

CONTENTS

Volume 2 - Issue 2

ARTICLES

**** 3D study of modelling and animation of Kayseri Gülük Mosque**

Ali ULVİ, Abdurahman Yasin YİĞİT 33

****A Deep learning integrated mobile application for historic landmark recognition: A case study of Istanbul**

Bulent Bayram, Batuhan Kilic*, Furkan Ozoglu , Firat Erdem , Tolga Bakirman, Sinan Sivri, Onur Can Bayrak , Ahmet Delen 38

**** Comparison of documentation cultural artifacts using the 3D model in different software**

Abdurahman Yasin Yiğit*, Yunus Kaya, Adem Kabadayı 51

**** Determination of pond volume with using an unmanned aerial vehicle**

Aydın Alptekin*, Murat Yakar 59

****Investigation of The Rainwater Harvesting Potential at the Mersin University, Turkey**

A. Yasin YİĞİT, Osman ORHAN*, Ali ULVİ



Mersin Photogrammetry Journal

<https://dergipark.org.tr/en/pub/mephoj>

e-ISSN 2687-654X



3D study of modelling and animation of Kayseri Gülük Mosque

Ali Ulvi ^{*1}, Abdurahman Yasin Yiğit ²

¹Mersin University, Remote Sensing and Geographic Information Systems, Mersin, Turkey

²Mersin University, Engineering Faculty, Geomatics Engineering Department, Mersin, Turkey

Keywords

Gülük Mosque
Close-range photogrammetry
Documentation
Kayseri
Cultural Heritage

ABSTRACT

The preservation of documents, which are described as cultural heritage, can be accepted as the common duty of delivery to future generations of humanity. In documenting the cultural heritage, the current state of historical monuments must first be determined. For this, various techniques are used in the literature. Recently, Close-range photogrammetry documentation of cultural heritage, which develops rapidly in line with technological developments, has an important place in the study. Documentation of close-range photogrammetry cultural heritage, which has developed rapidly in parallel with technological developments, has an important place in the studies. In this study, the study of documenting the Gülük Mosque in Kayseri/TURKEY with a photogrammetry technique was carried out. In this study, as a result, scaled drawings and three-dimensional model (3D) of the exterior of the mosque were obtained. Thanks to the photogrammetry technique, field and office work was completed in a short time according to classical documentation methods. With this method, works built throughout history can be archived with a 3D model in the digital environment. In addition, the 3D model obtained by the photogrammetry technique was animated and displayed in virtual museums.

1. INTRODUCTION

In Lands where Turkey is located, have lived thousands of civilizations throughout history. In this respect, Turkey has a rich cultural and historical heritage. According to the 2002 records of the Ministry of Culture and Tourism in Turkey registered 66 251 units in a single building scale cultural and natural heritage is available (URL-1).

At the same time, Turkey's Central Anatolia Region is an important center in terms of cultural artifacts. The number of registered buildings in Kayseri in this region is 829 according to the end of 2009 reports. 163 of these are religious structures (URL-1).

Documenting these works, conservation and needed to be restored, is of great importance in terms of cultural heritage studies. Cultural heritages are the history of nations, and history forms the identity of the nations. Therefore, the protection of cultural heritages means protection of the history and identity of the nations (Yakar and Doğan, 2017; Ulvi et al., 2019).

Documenting the cultural heritage process (Georgopoulos and İonnidis, 2004); " History or cultural structure of the set of three-dimensional space in the current situation, the new size, it is necessary to determine the shape and position measurement, assessment, recording, and presentation process " is defined as.

Various methods are used in the documentation of historical artifacts for different purposes. There are various methods such as classical manual inventory collection, topographic methods, photogrammetric methods and screening methods (Böhler and Heinz, 1999; Scherer, 2002). These methods provide great benefits to historical and cultural heritage objects in the future; The photogrammetry method used in this study includes scientific methodologies that calculate the three-dimensional coordinates of an object by measuring the corresponding points in the overlapping images (Akçay et al., 2017; Ulvi et al., 2020)

The most complex part of documenting cultural heritage seems to be to create three-dimensional modeling of these works. The close picture

* Corresponding Author

^{*}(aliulvi@mersin.edu.tr) ORCID ID 0000 - 0003 - 3005 - 8011
(ayasinyigit@mersin.edu.tr) ORCID ID 0000 - 0002 - 9407 - 8022

Ulvi A, Yiğit A Y (2020). 3D study of modelling and animation of Kayseri Gülük Mosque. Mersin Photogrammetry Journal, 2(2), 33-37

Cite this article

photogrammetry method was used for the easiest solution to this complex process. Close picture photogrammetry method; It is widely used in determining the structure of historical and archaeological value, making scale drawings of the building facade, preparing and implementing an urban conservation plan, cracks and deterioration analysis, damage assessment, restoration projects and in areas such as deformation detection studies (Yılmaz et al., 2000; Sienz et al., 2000).

In this study, the Mosque of Güllük documentation work is made with the close-range photogrammetric method. Detailed stone drawings were made on the exterior of the Güllük Mosque. In addition, a 3D model of the building was obtained and this model was presented as an animation on the virtual platform.

2. STUDY AREA

Güllük Mosque is located in the Güllük District of Kayseri, Melikgazi district. The Güllük Complex, built during the Danişmentlı period, consists of a mosque madrasa and a bath that is located next to them and is not available today (Figure 1).

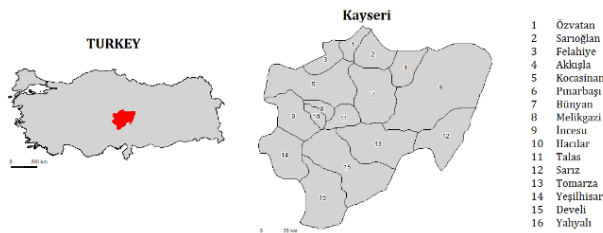


Figure 1. Güllük Mosque (Kayseri/TURKEY)

There is no epigraph that indicates the date and the construction of the complex or mosque. The older one of the two inscriptions on the building is on the crown gate on the northeast facade and added later. According to this inscription, the buildings were repaired in 1211 by the daughter of Yağıbasan Mahmut, Atsız Elti Hatun, the nephew of Sultan Mehmet Melik Gazi. This inscription on Taçkapı consists of three lines and the inscription of the inscription written with the Seljuk sulcus is as follows: "This building is the son of Keyhüsrev, the honor of the world and religion, the owner of the conquests, the partner of the Emir of the Believers, the time of the reign of the great Sultan Keykavus. Atsuz Elti Hatun, the weakest servant, chaste woman, daughter of Yağıbasan son Mahmud, repaired it in 607 (1210)"(URL-2).

The building has two lower and three upper windows on the south facade wall. One of these windows belongs to the upper and lower mosque section and the rest to the madrasah section. The lower window on the western facade belongs to the upper rooms of the two-story madrasa. The east facade wall has four rectangular windows 2.5 meters high on the floor. The north facade wall of the mosque is the front wall of the mosque and the madrasah. On this front, Taçkapı, located in the northeast and built by Atsuz Elti Hatun, has a mosque door 11 meters away from it (west) and an entrance door of the madrasa about 8 meters away from the mosque door. The courtyard of the mosque is bordered by three arches

and four feet of different apertures in the east and west directions, and the top is covered with a double-centered cradle vault as in the entrance section. 3.80x5.80 m in the middle of this vault. It has a rectangular opening. It was determined that there was an opening (skylight) in the middle of the mosque, which was first seen in Seljuk architecture. This opening was later converted into squares with additional arches to the east and west directions, and 3.60 m. The image of the restoration works of the building is shown in figure 2.



Figure 2. Güllük Mosque

3. METHODS

The handheld camera which does not have any special equipment was used in the study. The main goal in the use of the digital handheld camera in practice is to investigate the success of modeling historical artifacts with photographs taken by people without a special purpose.

The method used in the study is the photogrammetry method.

Photogrammetry is a method that allows the recreation of object properties without contact with the object (Krause, 2007).

Photogrammetry is an independent method in the documentation process. This method is based on at least two images with a sufficient amount of overlap between each other (Yakar & Doğan, 2017). Therefore, there is a need for at least two pictures taken from different angles of the object to be photogrammetry. In order to be successful, the first and most important stage of the object to be documented is the photographing stage. After photographing the object, measurement is done with a sensitive measuring device to scale the work to be done.

3.1 Field Studies

In the field study, the photos of the object to be documented are taken first. Photos of the historical building were taken with a Canon digital handheld camera. The digital handheld camera is shown in Figure 3. Technical features are shown in table 1.

After taking the photos, the detail points of the building should be measured. The purpose of this is that it is desired to form a more sensitive and real scale model of the building. Natural details, which can be easily distinguished in photographs, should be measured. Or, ready-made signboards in appropriate colors and forms should be placed and measured.

Measurements should be made with at least three detail points in each image (Burns et al., 2009). The number of detail points varies depending on the size of the surface. In the study, 32 detail measurements were made. Measurements were made with the Topcon GPT-3007 geodetic instrument shown in Figure 4.



Figure 3. Canon IXUS 180

Table 1. Canon IXUS 180 Technique Specifications (URL-3)

Canon IXUS 180	
Effective megapixels	20
Total megapixels	20.5
Sensor size size	1/2.3"
Max. image resolution	5152 x 3864
Crop factor/Optical zoom	5.62 / 10x
ISO	Auto, 100-1600
Focal length	24 - 240 mm
Max aperture	f3 - f6.9
Max. aperture	f16.9 - f38.8
Min. shutter speed	15 sec
Max. shutter speed	1/2000 sec
White balance presets	5
Screen size / resolution	2.7" / 230,400 dots
Max. video resolution	1280x720 (25p)
Weight	138 g
Dimensions	95.3 x 56.8 x 23.6 mm



Figure 4. Topcon 3007 Totalstation

3.2. Photogrammetric Work

After collecting the necessary data in the field study, office work started. In-office work, first of all, the detail points measured in the field are checked. Then, data is transferred to the necessary software to obtain a 3D model from 2D photos (Yakar et al., 2016).

In this study, PhotoModeler photogrammetric software was used for documentation study. PhotoModeler software is a Windows-based software program developed by EOS System. This software enables the digital images of an object to be used to obtain a three-dimensional model and to create a metric scale. In this three-dimensional software model; includes points, corners, and/or a series of curves.

Photos are first import to photogrammetric software (Figure 5). 56 photographs were used to model the Gülük Mosque. Then the detail points are marked on all pictures one by one and the photos are orientated.

All 56 photographs used in the study were balanced with 2.10 rms (Figure 6). After the photos were orientated, all the details of the building were drawn (Figure 7).

Finally, the real model and the surface were applied to the 3D model created as the basic structure (Figures 8 and 9). Then, the 3D model obtained was transferred to Sketchup software and the missing facades were completed (Figure 9).

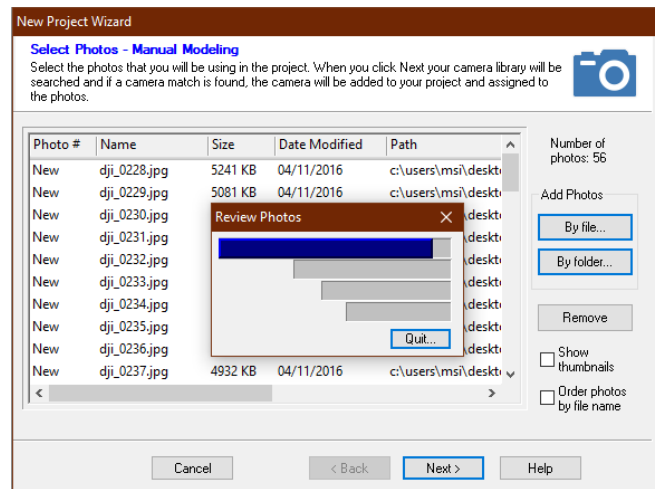


Figure 5. Photographs import to Software

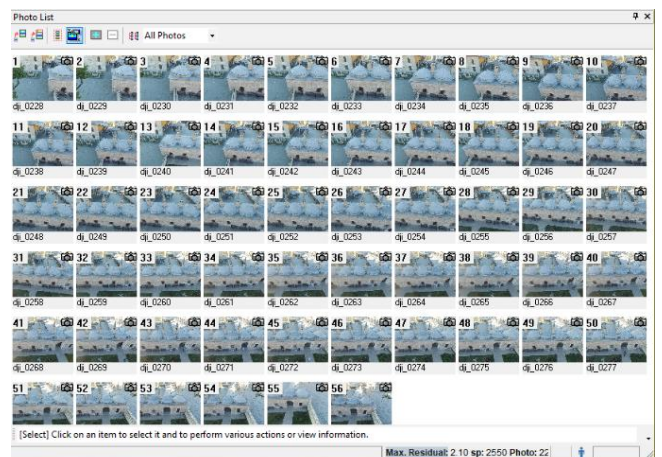


Figure 6. Result of oriented process

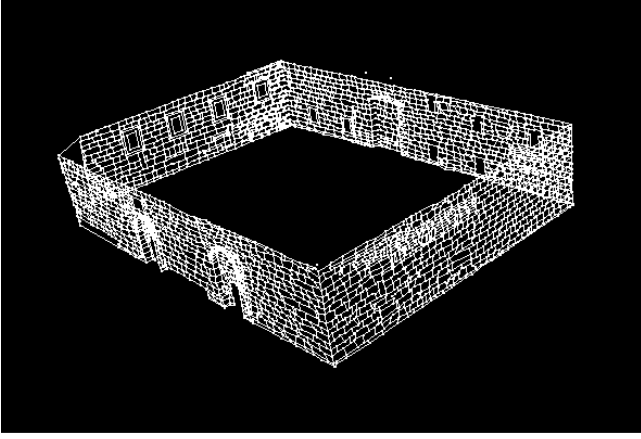


Figure 7. Güllük mosque 3D model



Figure 8. Textured model of Güllük Mosque

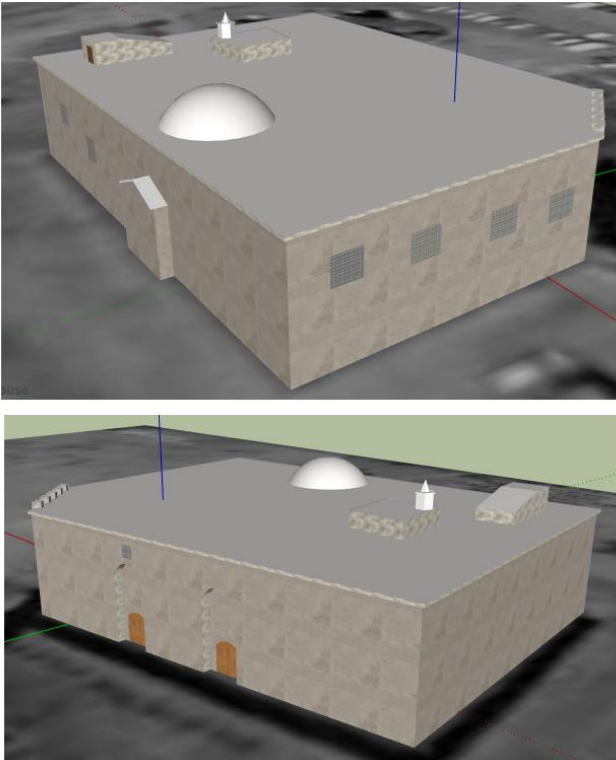


Figure 9. Adding top façades in Sketchup software

4. CONCLUSION

Cultural heritage documentation is a very important issue in terms of human history. It needs to be protected due to neglect and indifference or the destruction of a large part of these artifacts for various reasons. Creating a digital archive is of great importance in order to restore the damaged structures.

Close-range photogrammetry showing great improvement in parallel with the rapid advances in

computer also effective when used in the documentation of cultural heritage and is a very efficient method. Drawing at the desired scale of the structure of cultural heritage, taking advantage of the opportunities provided by the current technology in the creation of 3D models can be made quickly and accurately by close-range photogrammetry. The original image 3D model can be obtained by adding texture data with the close-range photogrammetry method. 3D models obtained in the digital platforms are used especially in restoration works. Documentation works for the protection of cultural heritage provide great benefits in a short time and economically with the photogrammetric method.

It is impossible to model the photographs taken with the close-range photogrammetry technique because they do not have upper facades. Such deficiencies resulting from the shooting location of the camera can be corrected by taking new photos from different locations. For example, this deficiency can be overcome by using platforms that enable shooting from the air, such as unmanned aerial vehicles (UAV), which have been preferred by many disciplines recently.

REFERENCES

- Akçay, O., Erenoglu, R C., Avsar, E O. (2017). The effect of jpeg compression in close range photogrammetry. *International Journal of Engineering and Geosciences (IJEG)*, 2 (1) , 35-40.
- Böhler, W. and G. Heinz. (1999). Documentation, surveying, photogrammetry. *XVII CIPA Symposium*, Recife, Olinda.
- Burns, J. C., Stone, K. C., Hunt, P. G., Vanotti, M. B., Cantrell, K. B. and Fisher, D. S. (2009). Intake and digestibility of 'Coastal' Bermudagrass hay from treated swine waste using subsurface drip irrigation. *J. Environ. Qual.*, 38 (4): 1749-1756.
- Kraus, K. (2007). Fotogrametri, Fotoğraflardan ve Lazer Tarama Verilerinden Geometrik Bilgiler, Translate, İTÜ, (Translated, M.O.Altan et. all.)
- Scherer, M. (2002). About the synthesis of different methods in surveying. *XVIII International Symposium of CIPA*, Posdam, Germany, 2002.
- Sienz J., Szarvasy I., Hinton E. and Andrade M.L. (2000). Copputational modelling of 3D objects by using fitting techniques and subsequent mesh generation, *Computers and Structures* 78, 2000, 397-413.
- Ulvi, A., Yakar, M., Yiğit, A. and Kaya, Y. (2019). The Use of Photogrammetric Techniques in Documenting Cultural Heritage: The Example of Aksaray Selime Sultan Tomb. *Universal Journal Of Engineering Science*, 7(3), 64-73.
- Ulvi, A., Yakar, M., Yiğit, A. Y. and Kaya, Y. (2020). İHA ve Yersel Fotogrametrik Teknikler Kullanarak Aksaray Kızıl Kilise'nin 3 Boyutlu Nokta Bulutu ve Modelinin Üretilmesi. *Geomatik Dergisi*, 5(1), 22-30.
- Yakar M., Yılmaz H. M., Yıldız F., Zeybek M., Şentürk H., and Çelik H. (2009). Silifke-Mersin Bölgesinde Roma Dönemi Eserlerinin 3-Boyutlu Modelleme Çalışması ve Animasyonu, TMMOB Harita ve Kadastro Mühendisleri Odası 12. Türkiye Harita Bilimsel ve Teknik Kurultayı, 11-15 Mayıs 2009, Ankara.

Yakar, M., Kabadayı, A., Yiğit, A. Y., Çıkıkcı, K., Kaya, Y. and Catin, S. S. (2016). Emir Saltuk Kümbeti Fotogrametrik Rölöve Çalışması ve 3Boyutlu Modellenmesi. *Geomatik*, 1(1), 14-18.

Yılmaz H. M., Karabörk H. and Yakar M. (2000). Yersel Fotogrametrinin Kullanım Alanları, *Niğde Üniversitesi Mühendislik Bilimleri Dergisi*, 4, 2000, 18-28.

URL-1. <https://www.ktb.gov.tr/> (Retrieved: 01.15.2020)

URL-2. <http://www.kayseri.gov.tr/guluk-cami> (Retrieved: 01.12.2020)

URL-3. https://www.digicamdb.com/specs/canon_ixus-180/ (Retrieved: 01.14.2020)



© Author(s) 2020. This work is distributed under <https://creativecommons.org/licenses/by-sa/4.0/>



A Deep learning integrated mobile application for historic landmark recognition: A case study of Istanbul

Bulent Bayram ¹, Batuhan Kilic*¹, Furkan Ozoglu ², Firat Erdem ³, Tolga Bakirman ⁴, Sinan Sivri ⁴, Onur Can Bayrak ¹, Ahmet Delen ⁵

¹ Yildiz Technical University, Civil Engineering Faculty, Department of Geomatic Engineering, Istanbul, Turkey

² Istanbul Metropolitan Municipality, Directorate of Geographic Information Systems, Istanbul, Turkey

³ Eskisehir Technical University, Earth and Space Sciences Institute, Eskisehir, Turkey

⁴ Istanbul Technical University, Research and Application Center for Satellite Communications and Remote Sensing, Istanbul, Turkey

⁵ Gaziosmanpasa University, Department of Geomatic Engineering, Tokat, Turkey

Keywords

Deep learning
Convolutional Neural
Network (CNN)
Historic landmark
recognition
Mobile technology

ABSTRACT

Recent developments in mobile device technology and artificial intelligent systems took the attention of many researchers. Historical sites and landmarks are the indispensable heritage of cities. Historic landmark recognition, including detailed attribute information, can connect people directly with the history of the cities, although they may not be familiar with the impressive historical monument. This can be achieved by integrating mobile and deep learning technologies. Therefore, we focused on establishing a deep learning (DL) based mobile historic landmark recognition system in this study. The VGG (16, 19), ResNet (50, 101, 152), DenseNet (121, 169, 201) DL architectures were trained by end-to-end learning techniques for the recognition of ten historic landmarks from the metropolitan city of Istanbul, Turkey. The dataset was prepared by collecting images of ten historical buildings from the image hosting services. The developed prototype automatically and instantly recognizes these historic landmarks from scene images and immediately provides related historic information as well as route planning. The experimental results indicate that DenseNet-169 architecture is very effective for our dataset with 96.3% accuracy. This study has shown that deep learning offers a promising alternative means of recognizing historic landmarks.

1. INTRODUCTION

Istanbul is one of the most significant metropolitan cities in the world. This city, which hosts the unique signs of European and Asian communities through Byzantine and Ottoman cultural heritage, has been named as the 2010 European Capital of Culture due to its unique historic areas that attract many visitors (UNESCO, 2006).

Tourism is the name given to trips to an unknown place (Brown, 2007; Mulazimoglu and Basaraner, 2019). Visitors aspire to discover and witness the varied life of the city (Richards, 2018). In this respect, landmarks, known as recognizable natural or artificial features, often

attract people to visit and create memories to share with their social group. Sometimes during a trip, unknown historical objects can attract attention (Cheng and Shen, 2016). However, they can only interact visually with cultural objects without detailed information. This situation results in a limited awareness of cultural heritage. To improve visitors' experience, rapid, accurate, significant, and real-time information is needed.

The growing use of social networks has provided large amounts of data relating to every field. This has brought new opportunities for concept-based image recognition (Simonyan and Zisserman, 2014). People

Cite this article

* Corresponding Author

(bayram@yildiz.edu.tr) ORCID ID 0000-0002-4248-116X
*(batuhank@yildiz.edu.tr) ORCID ID 0000-0002-0529-8569
(furkan.ozoglu@ibb.gov.tr) ORCID ID 0000-0002-6276-3762
(firaterdem@eskisehir.edu.tr) ORCID ID 0000-0002-6163-1979
(tolga@cscrs.edu.tr) ORCID ID 0000-0001-7828-9666
(sinan@cscrs.edu.tr) ORCID ID 0000-0002-8591-9555
(onurcb@yildiz.edu.tr) ORCID ID 0000-0002-5147-747X
(ahmet.delen@gop.edu.tr) ORCID ID 0000-0003-3091-8501

Bayram B, Kilic B, Ozoglu F, Erdem F, Bakirman T, Sivri S, Bayrak O C & Delen A (2020). A Deep learning integrated mobile application for historic landmark recognition: A case study of Istanbul. Mersin Photogrammetry Journal, 2(2), 38-50

have started voluntarily to share their images using different social media applications such as Flickr, Facebook, and Instagram (Weyand and Leibe, 2015) and internet search engines. A variety of studies and applications have been carried out, investigating location estimation (Hays and Efros, 2008), scene recognition (Zhou et al., 2018), face recognition (Parkhi et al., 2015) and landmark recognition (Cheng and Shen, 2016), using images taken from these kinds of a large database.

The enhancement and promotion of cultural heritage using information and communication technologies are an essential research issue (Amato et al., 2017; Şasi and Yakar, 2018). Although human-computer interaction and mobile digital technology have the potential to provide to access cultural heritage information (Doğan and Yakar, 2018; McGookin et al., 2019), existing frameworks may not be capable of presenting smart and detailed data. The state-of-art DL techniques brought new opportunities to overcome this problem. DL is based on multi-layer Artificial Neural Network (ANN) and a subset of machine learning. It has been confirmed in many studies such as computer vision, image classification, robotics, bioinformatics, biomedical, geomatics (Zhang et al., 2018) that DL has become a handy tool for image and information analysis, primarily using open databases and internet resources (Tzelepi and Tefas, 2018).

Jiang et al. (2017) developed a real-time internet cross-media retrieval system using DL. Shukla et al. (2017) proposed a deep convolutional neural networks model for the recognition of 117 Indian monuments. Termritthikun et al. (2018) proposed a DL network named as NU-LiteNet for mobile landmark recognition.

Huang et al. (2018) proposed DL as a tool to solve multi-concept-based image retrieval problems using MIR Flickr 2011 and NUS-WID dataset. F. Huang et al. (2018) combined content and network for multi-view learning and proposed a deep multi-view embedding model-based image recognition system. Xu et al. (2019) used the same dataset and developed a unimodal semantic image retrieval system using DL techniques.

As can be seen from the literature review, there is limited study concerning DL for mobile historic landmark recognition. Therefore, the objective of this study is to test the efficiency of different DL architectures for mobile historic landmark recognition. For this purpose, the Visual Geometry Group (VGG16, 19) (URL1), Deep Residual Network (ResNet-50, 101, 152) (URL2), and Densely Connected Convolutional Network (DenseNet-121, 169, 201) (URL3) architectures were exploited to recognize ten selected historic landmarks in Istanbul, Turkey. All utilized DL architectures have been trained and tested with our generated dataset.











2. STUDY AREA AND DATASET

The generated dataset consists of the most popular and essential ten historic landmarks within the boundaries of Istanbul. These are the Maiden's Tower, the Sultan Ahmet Mosque (Blue Mosque), the Galata Tower, Hagia Sophia, the Ortaköy Mosque, the Topkapi Palace, the Valens Aqueduct, the Dolmabahce Palace, the Obelisk of Theodosius, and the Dolmabahce Clock Tower (Table 1). The distribution of landmarks can be seen in Figure 1.



Figure 1. Distribution of landmarks

Table 1. Samples of the selected historical landmarks

Landmarks	Construction	Name	Description
1 	Stone (concrete) tower, masonry cupola	Maiden's Tower	It is built up on the rock, 200 meters from the coast of Üsküdar, Istanbul, on the Bosphorus. It was built around 419 BC (IPDCT, 2019a).
2 	Mosque (Islamic, Late Classical Ottoman)	Blue Mosque	This unique mosque in Istanbul has six minarets and eight domes. It was built by Sedefkar Mehmet Aga between 1609–1616 (IPDCT, 2019b).
3 	Stone tower	Galata Tower	It was built in the 14th century by the Genoese (IPDCT, 2019c).
4 	Mosque (museum)	Hagia Sophia	It was built between 537 and 537 AD and was famous in particular for its massive dome (IPDCT, 2019d).
5 	Mosque (Baroque Revival)	Ortaköy Mosque	It was built in 1853 by architect Karabet Balyan and was then repaired between 1960 and 1972 (IPDCT, 2019e).
6 	Palace (Various low buildings, surrounding courtyards, pavilions and gardens)	Topkapi Palace	It was built between 1466 and 1478 by the sultan Mehmet II. The palace was the political centre of the Ottoman Empire between the 15th and 19th centuries (IPDCT, 2019f).
7 	Arch bridge (stone, brick)	Valens Aqueduct	It is part of Istanbul's ancient water supply system and was built in the late 4th century AD during the reign of Roman Emperor Valens (Yorulmaz and Çelik, 2015).
8 	Palace (Baroque, Rococo, Neoclassical)	Dolmabahçe Palace	It was built by order of Sultan Abdulmecid I between 1843 and 1856 (IPDCT, 2019g).
9 	Column (granite)	Obelisk of Theodosius	The obelisk was built by Pharaoh Thutmose III (1479–1425 BC) during the 18th dynasty (IPDCT, 2019h).
10 	Clock tower (Ottoman Neo-Baroque)	Dolmabahçe Clock Tower	Built in 1890–1895, by palace architect Sarkis Balyan II. It was built for Sultan Abdulhamid between 1842–1918 (IPDCT, 2019i).

Two different datasets were prepared to train all the selected DL architectures from the Bing, Foursquare, and Yandex web platforms. The first one (Istanbul-2500) consisted of 2500 images and the second one (Istanbul-5000) 5000 images of all selected historic landmarks. In addition to the online image resources, 310 new images were taken in the field for the Istanbul-5000 dataset. The images which have the same width and height were selected to avoid possible image deformations and resized to 224 x 224 pixels as input dimensions of used DL architectures.

3. METHODOLOGY

Due to their proven success in the ImageNet Large Scale Visual Recognition Challenge (ILSVRC) (Deng et al., 2012), the VGG (16 and 19) (Simonyan and Zisserman, 2014), ResNet (50, 101 and 152) (He et al., 2016a), and DenseNet (121, 169 and 201) (Huang et al., 2017) DL architectures were utilized for this study. These DL architectures have also been used in many other image

classification studies (Nawaz et al., 2018; Nibali et al., 2017; Rothe et al., 2018). All the used architectures were tested for recognition of selected historic landmarks. Our mobile application was integrated with the DL architecture that gave the best accuracy. A flowchart of the study is given in Figure 2.

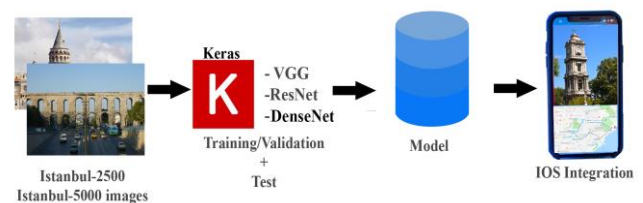


Figure 2. The flowchart of the study

3.1. Implementation of Different Deep Learning Architectures

The details of all the deep CNN architectures employed for historical object recognition using the

Istanbul-2500 and Istanbul-5000 datasets are given below:

3.1.1. VGGNet

The VGG neural networks were developed by the Visual Geometry Group. There are four different versions of the VGG neural networks, which include different weight layers of 11, 13, 16, and 19, respectively (Simonyan and Zisserman, 2014). In this study, the VGG16 and VGG19 versions were employed. The VGG neural networks consist of convolution, pooling, and fully-connected layer and softmax layers. The filter kernel size in the convolution layers is 3 x 3. The rectified linear unit (ReLU) activation function is applied for the nonlinearity process after each convolution layer. After each convolution layer, there are a max-pooling layer with 2 x 2 window sizes (Patterson and Gibson, 2017). In the pooling layers, the shifting interval of the filter is defined by a stride parameter. The stride parameter for VGG neural networks is defined as two. Three fully-connected layers and Softmax classifier layers are used in the last part of the architecture. The first two fully-connected layers have 4096 channels. Dropout regularization is applied in these layers to avoid overfitting problems. A dropout ratio of 0.5 is selected. The amount of the channels in the last fully-connected layer is equal to the count of the classes (Simonyan and Zisserman, 2014). The structures of the VGG architectures used in this study are given in Figure 3.

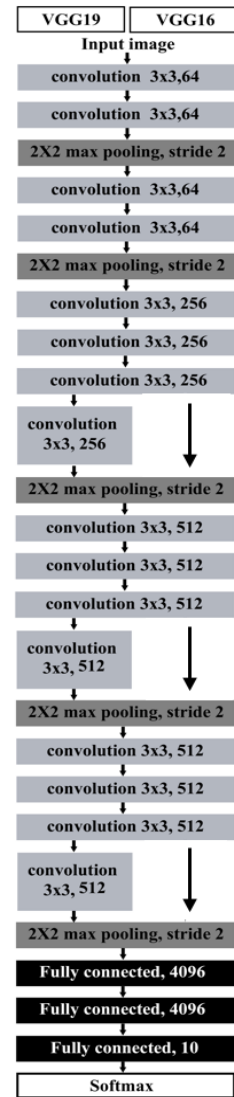


Figure 3. VGG16 and VGG19 layers (Simonyan and Zisserman, 2014)

3.1.2. ResNet

ResNet was developed by the Microsoft research team to reduce the training difficulty of deeper neural networks. The main idea of ResNets is to learn the additive residual function using an identity mapping by using short connections (He et al., 2016b). It has versions consisting of 18, 34, 50, 101, and 152 weight layers (He et al., 2016a). Instead of learning non-discriminatory functions in ResNet architectures, residual functions are adopted using input layers. Unlike VGG, ResNet architectures have shortcut connections which are used in feed-forward neural networks. Thus, shortcut links do

not contain extra parameters and do not cause computational complexity. In this way, relevant information from the previous layer can be transferred to the next layers (He et al., 2016b).

In contrast to VGG architectures, ResNet architectures contain a global average pooling layer and a fully connected layer at the end of the network. Without a dropout operation, the average value in each property map is transferred to the next layer in the global average pooling process (Lin et al., 2013). The parameters of the ResNet layers used in this study are given in Figure 4.

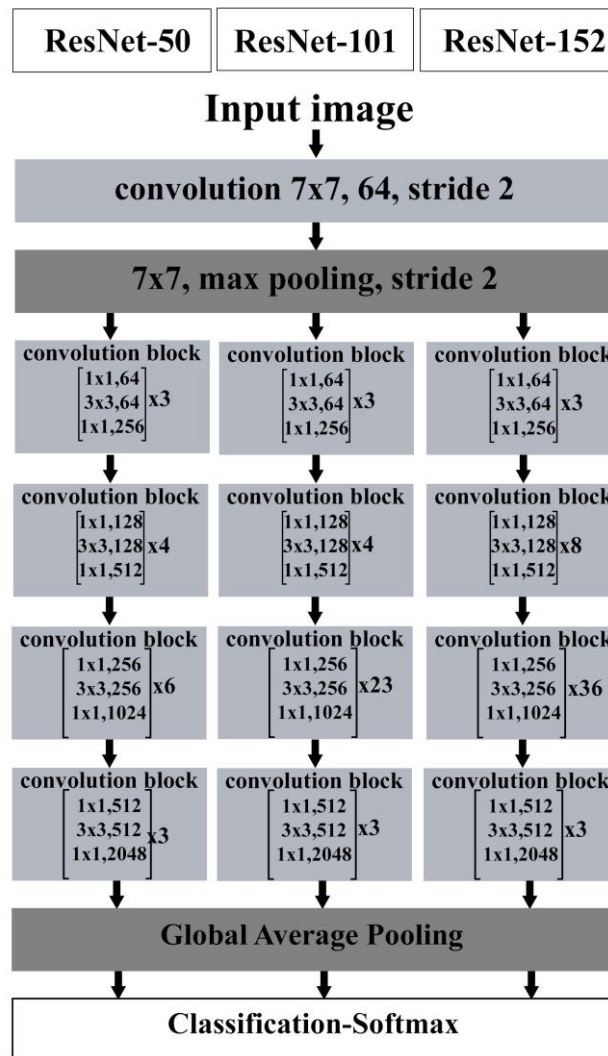


Figure 4. ResNet50, ResNet101 and ResNet152 layers (He et al., 2016a)

3.1.3. DenseNet

DenseNet is well known CNN architecture. Individual layers are connected with every layer behind it. Thus, all layers are used for a decision instead of the single final layer by CNN. DenseNet has been developed by the inspiration of ResNet18 architecture, which is one of the best deep learning architecture and used in many different image classification related studies. Compared to ResNet architecture, it has been seen that if shorter connections between layers close to the input and layers close to the output, the training accuracy can be obtained more accurate. DenseNet architecture is based on the feed-forwarded connection of each layer to every other layer to extend the shorter connections. By DenseNet, feature propagation is reinforced, the amount of parameters is diminished (Gunawan et al., 2018).

DenseNet also has different versions, consisting of 121, 169, 201, and 264 weight layers. Similarly to ResNets, DenseNets use a block concept, too. Unlike ResNets, the principle of intense connections is used in the blocks, according to which each layer in a block has a connection with the previous layers. These connections are provided by transferring feature maps. There are convolution and pooling layers between the blocks. In DenseNet architectures, except for the first convolution layer, dropout is applied with a 0.2 dropout rate after each convolution layer. In addition to this, the ReLU activation function is used following the convolution layers (Huang et al., 2017). The parameters and structure of DenseNet architectures can be seen in Figure 5.

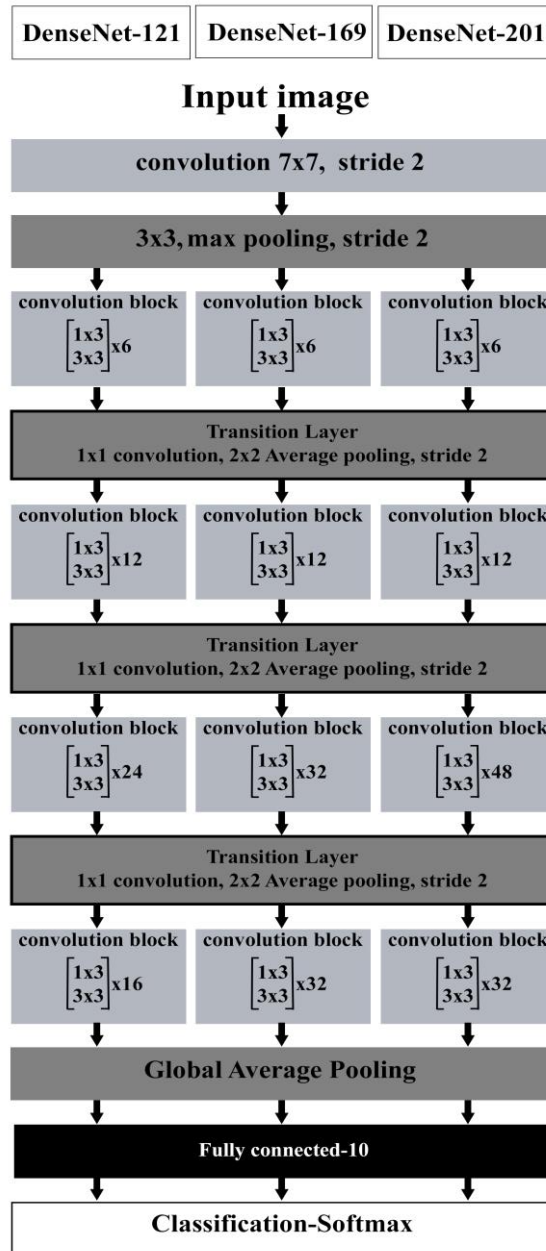


Figure 5. DenseNet121, DenseNet169 and DenseNet201 layers (Huang et al., 2017)

Table 2. Used hyperparameters

Deep Learning Models	Base Learning Rate	Rho	Epsilon	Decay	Epoch	Mini-Batch Size
VGG16	0.05	0.95	1e-07	0	120	16
VGG19						
ResNet50	1	0.95	1e-07	0	120	16
ResNet101						
ResNet152						
DenseNet121						
DenseNet169						
DenseNet201						

Used hyperparameters are given in Table 2. The base (initial) learning rate affects the optimization parameters in order to minimize CNN estimation errors. ρ is a constant, which controls the decay of parameter updates (Patterson and Gibson, 2017). Epsilon is a floating-point number and very close to zero. It is used to prohibit mistakes similar to dividing by zero. Decay is the

rate of initial learning (Keras, 2019). Epoch is the number of training iterations (Patterson and Gibson, 2017). The mini-batch size is the number of records that are passed into a defined learning algorithm at the same time (Soon et al., 2018). Components of used hardware and software specifications can be seen in Table 3.

Table 3. Specifications of hardware and software used

Hardware			
Computer	Desktop PC	MacBook Pro Retina (Mid 2012)	
CPU	Intel® Core™ i7-8700K 3.7GHz	Intel® Core™ i7-3615QM 2.3GHz	
Display Card	NVIDIA GeForce GTX1080Ti 11 GB	NVIDIA GeForce GT 650M 1 GB	
Memory	32 GB	8 GB	
Software			
Library	Tensorflow	Keras	CoreML
Version	1.5.0	2.1.3	2.0

3.2. Integration of the Mobile Application

The iOS platform, one of the most popular mobile application platforms in the world, is continuously being updated for iPhone and iPad devices. The CoreML framework structure developed by Apple for machine-learning applications was announced to developers in 2017 (CoreML Framework, 2019). Also, the CoreML tools that work with Python were used to transfer other machine and DL frameworks (i.e., Keras, Tensorflow, IBMWatson) to mobile applications (CoreML Documentation, 2019). The Vision Framework is integrated with the CoreML library and is used to define images via a mobile application (Maskrey & Wang, 2018). The free Mapkit Framework library was developed by Apple to create map-based mobile applications (MapKit Framework, 2019). It has two modes, namely standard, and satellite. The Core Location Framework (Core

Location Framework, 2019) works by being integrated with the GNSS receiver on a mobile device. The device’s location can be seen on the map when it is used with MapKit. The mobile phone integration flowchart is given in Figure 6. The application for mobile phone integration was developed by Xcode 10 IDE (Integrated Development Environment) using the Swift 4.2 environment. The developed application only works with iPhone instruments and supports iOS Versions 10.0–13.0. In addition to the integration of the Vision, Core Location and MapKit frameworks to allow the use of trained deep CNN models offline, the mlmodel was created for mobile phones by exploiting the CoreML framework. However, for route planning and location definition, the navigation services in the application need access to a network (3G/4G) or WiFi connection.

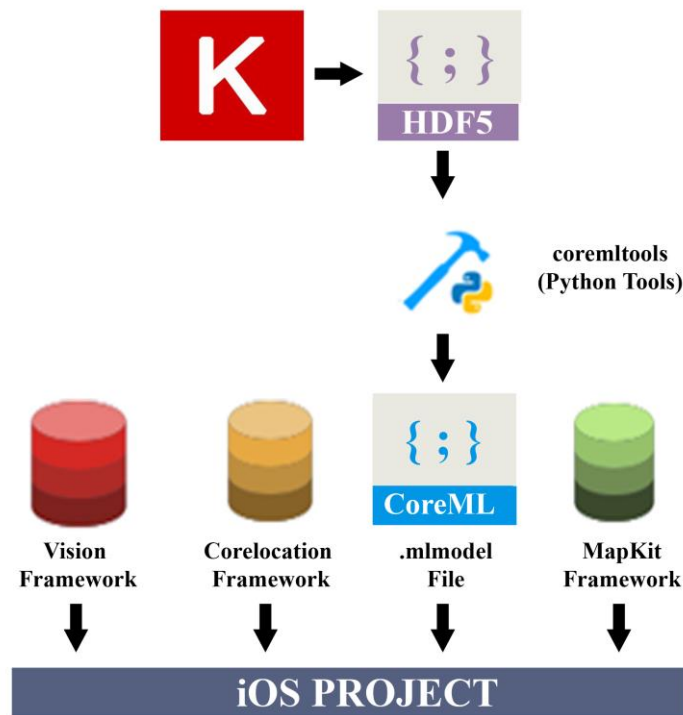


Figure 6. Mobile integration flowchart

4. RESULT AND DISCUSSION

In this study, we investigated the performance of 8 deep CNN architectures (VGG16, VGG19, ResNet50, ResNet101, ResNet152, DenseNet121, DenseNet169

and DenseNet201) for mobile historic landmark recognition. Python’s Keras library (Chollet, 2015) was used to implement all of the selected deep CNN

architectures. 70% of the dataset was used for training, 10% for validation, and 20% for testing. The highest test accuracy was achieved by the DenseNet169 architecture for the Istanbul-5000 dataset (96.3%).

The robustness of the optimization algorithms is still controversial, and there is no consensus regarding the optimal optimization algorithms among experts (Schaul et al., 2014). Therefore, training of the deep CNNs was carried out using the Adadelta optimization algorithm. This method uses only first-order information during dynamical adaption and minimal computational cost. It is robust to noisy gradient

information and accommodates a selection of hyperparameters (Zeiler, 2012).

The training/validation accuracy for each epoch was compared to evaluate the training. Therefore, the training accuracy of each deep CNN architecture and dataset were analysed separately. As can be seen in Figure 7, the test accuracy for VGG16 and VGG19 with two datasets reached a maximum of around 80%. This shows that the VGG16 and VGG19 architectures are unable to produce a comprehensive solution for this study.

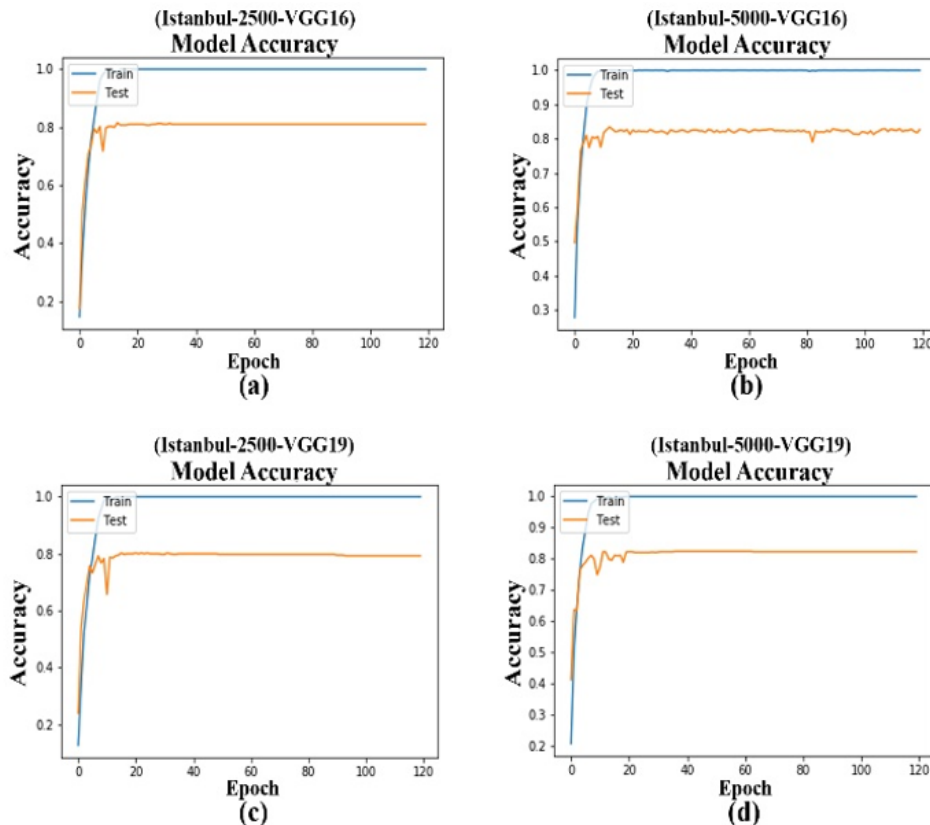


Figure 7. VGG16 and VGG19 training results for the Istanbul-2500 and Istanbul-5000 datasets

The training results for the ResNet architectures (50, 101, and 152) were much noisier than those for the DenseNet models (Figure 8 and Figure 9). It has been observed that, in the epochs where the accuracy of training increased, the test accuracy showed opposite directions for all ResNet architectures on both datasets. However, in general, in the epochs where training was completed, training and test accuracies converged (Figure 8). As a result, the calculated accuracies for the ResNet architectures were similar to those for the VGG architectures.

The evaluation of the training/test accuracies for the DenseNet architectures (121, 169, and 201) for the Istanbul-2500 and Istanbul-5000 datasets are given in Figure 9. A more stable training/test accuracy was observed for DenseNet-169 for the Istanbul-5000 dataset (Figure 9e) than for all the other DL models used. After the 100th epoch for both the DenseNet169 and DenseNet201 architectures and the Istanbul-5000 dataset, the large fluctuations stabilized, and the test accuracies converged to the training accuracy. It should be mentioned that the model architecture and the dataset size are compatible.

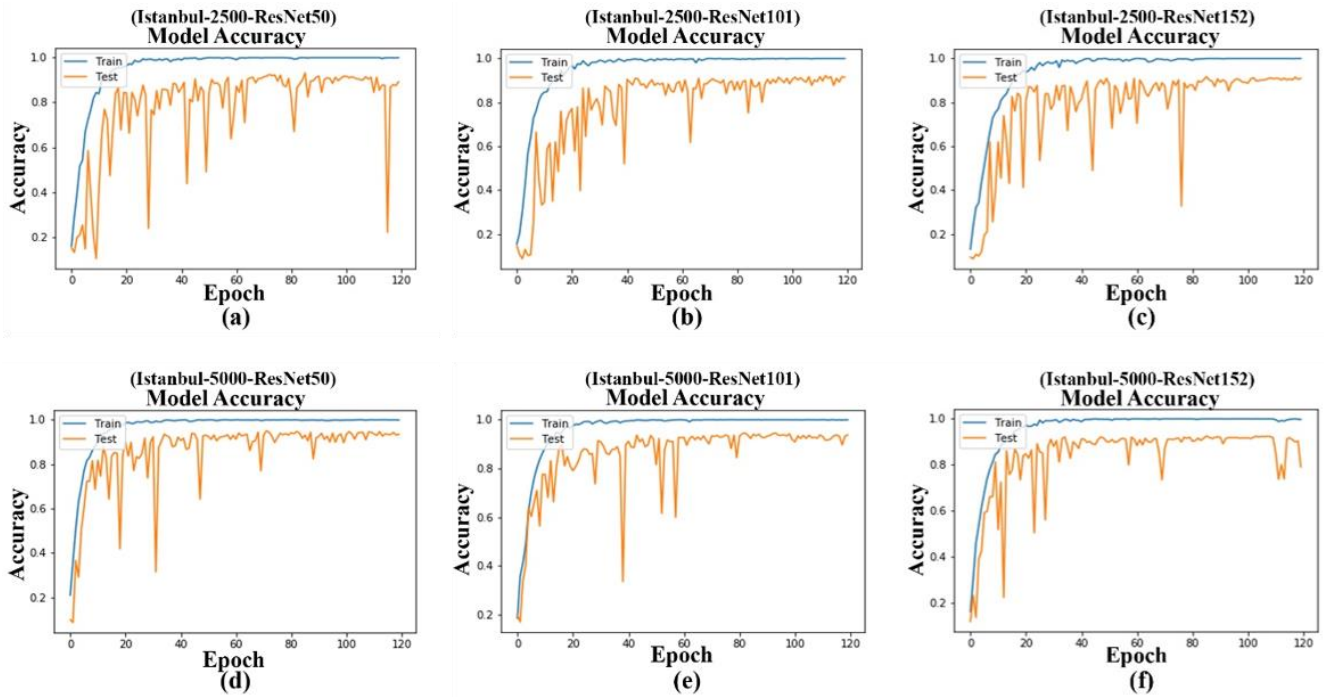


Figure 8. ResNet50, ResNet101 and ResNet152 training results for the Istanbul-2500 and Istanbul-5000 datasets

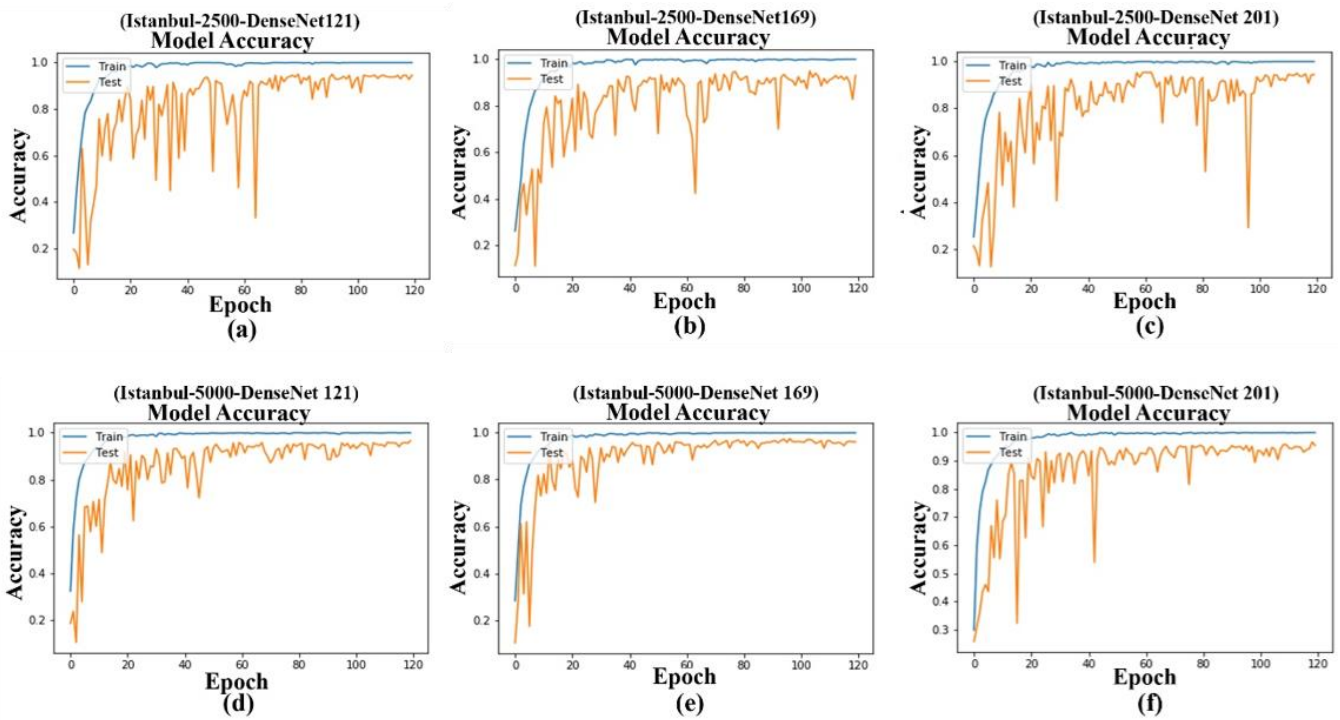


Figure 9. DenseNet121, DenseNet169 and DenseNet201 training results for the Istanbul-2500 and Istanbul-5000 datasets

In this study, precision, recall, and F1-Score metrics were used to analyze the results (Table 4). For the Istanbul-2500 dataset, the DenseNet architecture, which was able to evaluate feature maps from more layers, achieved a high level of success in all evaluation criteria for test accuracy, precision, recall, and F1-Score.

Except for ResNet-152, the mean accuracy results of the ResNets were higher than for VGG-16 and VGG-19. However, as with the VGG16 and VGG19 architectures, the accuracy results for the ResNets were found to be unsatisfactory for this study.

Table 4. Accuracy assessment results for the Istanbul-2500 and the Istanbul-5000 datasets

Deep Learning Architectures	Test Accuracy (%)		Average Precision (%)		Average Recall (%)		Average F1-Score (%)	
	Istanbul-2500	Istanbul-5000	Istanbul-2500	Istanbul-5000	Istanbul-2500	Istanbul-5000	Istanbul-2500	Istanbul-5000
VGG16	81	83.1	81.61	83.23	81	83.1	81.07	83.11
VGG19	82	83.6	82.57	83.76	82	83.6	82.07	83.61
ResNet50	90.2	93.2	91.2	93.43	90.2	93.2	90.29	93.22
ResNet101	91.6	92.4	92.32	92.46	91.6	92.4	91.68	92.41
ResNet152	90.6	81.4	91.17	85.21	90.6	81.4	90.68	81.37
DenseNet121	93.6	96.1	93.74	96.12	96.6	96.1	93.62	96.1
DenseNet169	91.8	96.3	92.23	96.35	91.8	96.3	91.88	96.3
DenseNet201	93.6	94.4	93.87	94.71	93.6	94.4	93.92	94.41

For both the Istanbul-2500 and Istanbul-5000 datasets, the superiority of the DenseNet-based architectures is conspicuous. The highest accuracy was obtained with the DenseNet-169 variant for all metrics. The test accuracy, average precision, average call, and F1-score results were calculated as 96.3%, 96.35%, 96.30%, and 96.3%, respectively. The confusion matrix for the DenseNet-169 results has been given in Table 5.

According to our results, the DenseNet-169 architecture was more successful than the other implemented DL architectures. Although the layer number of DenseNet-201 is higher than DenseNet-169, a lower accuracy was achieved compared to DenseNet-169. The reason for this situation might be related to the number of training images in the dataset.

Table 5. Confusion matrix for landmarks obtained from the DenseNet169 network

Landmarks	1	2	3	4	5	6	7	8	9	10
1	0.98	0	0.01	0	0	0	0	0	0	0.01
2	0.01	0.97	0	0	0	0	0.01	0	0	0.01
3	0.03	0.01	0.96	0	0	0	0	0	0	0
4	0	0.03	0.01	0.96	0	0	0	0	0	0
5	0	0.01	0.01	0	0.97	0	0	0.01	0	0
6	0	0	0	0.01	0	0.98	0	0	0	0.01
7	0	0	0	0	0	0	0.98	0	0.01	0.01
8	0.02	0	0.01	0.01	0.01	0	0	0.95	0	0
9	0	0	0.01	0	0	0	0.01	0	0.97	0.01
10	0	0.02	0.02	0	0	0	0.03	0.01	0.01	0.91

According to Table 5, the lowest accuracy was calculated for the Dolmabahce Clock Tower (Landmark 10) at 91%. Although the similarity between the Maiden's Tower (Landmark 1) and the Galata Tower (Landmark 3) is very high, there were no mix-ups in their recognition, as demonstrated by their results (which were 98% and 96%, respectively). Similarly, encouraging results were obtained for the Blue Mosque (Landmark 2),

Hagia Sophia (Landmark 4), and the Ortaköy Mosque (Landmark 5).

The training times for the eight DL architectures are given in Table 6. It can be seen that the training time of the ResNet-152 model for the Istanbul-5000 dataset was the longest. In contrast, ResNet-50 required minimum training time. The training time of DenseNet-169, which provided the best accuracy, was the third shortest of all the models.

Table 6. Training times of deep learning models

Istanbul-2500		Istanbul-5000	
ResNet50	0 h 38 m 54 s	ResNet50	1 h 18 m 43 s
DenseNet121	0 h 44 m 39 s	DenseNet121	1 h 29 m 45 s
DenseNet169	0 h 57 m 16 s	DenseNet169	1 h 53 m 10 s
VGG16	0 h 58 m 36 s	VGG16	1 h 57 m 31 s
DenseNet201	1 h 10 m 11s	VGG19	2 h 13 m 18 s
ResNet152	1 h 36 m 59 s	ResNet101	2 h 13 m 54 s
VGG19	1 h 6 m 59 s	DenseNet201	2 h 19 m 19 s
ResNet101	1 h 7 m 3 s	ResNet152	3 h 13 m 15 s

The Apple iOS mobile application was developed by integrating the weight file of the DenseNet169 architecture into the CoreML (.mlmodel), which can also work offline mode. The application uses either freshly taken images useful pre-existing photos on the phone. The system lists the three most probable of the ten

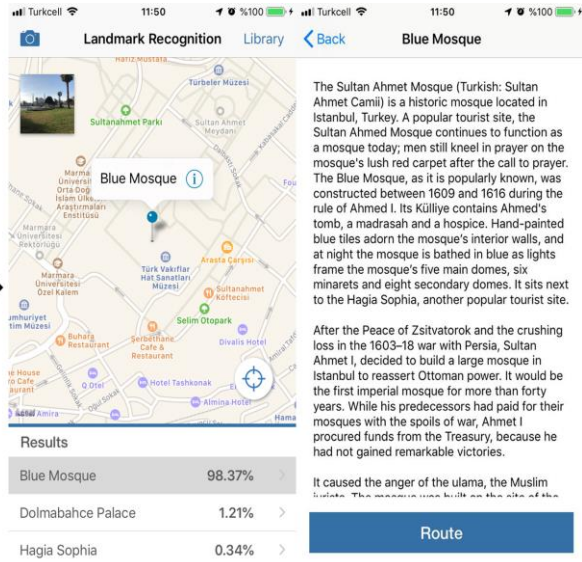


Figure 10. DL-integrated iOS-based mobile application

5. CONCLUSION

In recent years, DL architectures have been employed for different image vision and recognition studies. While some researchers have used existing DL architectures, some have developed DL architectures focusing on specific problems.

Historic landmarks, along with attribute information, are a challenging problem. It is possible to create smart systems using crowdsourcing data thanks to DL techniques. In this study, we investigated the efficiency of the DL technique for mobile historic landmark recognition. For this purpose, we explored eight different deep learning approaches to recognize ten historic landmarks of Istanbul. The highest F1-scores calculated for the DenseNets. The reasons for this could be related to the high linear and textural complexity of the selected historic objects and the number of classes. Our results show that deep learning offers a promising alternative means of recognizing historic landmarks.

The ten selected historic landmarks are unique monuments in Istanbul, and each has different textures and structures. Thus, it was possible to collect different characteristic images of the selected landmarks to generate training and test datasets. Only daylight images were included in this study. The developed framework can be extended for other historical landmarks in different cities around the world by collecting a more massive amount of data and working with more suitable computer configurations.

The proposed prototype can be used efficiently in Istanbul, which has an enormous amount of historical monuments. This system provides not only historic

included historical buildings after recognition, as well as their probabilities. The most probable structure can be selected by the user, and the system provides the location and route plan on the screen using GPS information from the phone (Figure 10).

landmark recognition but also attribute information and route planning. The developed mobile historic landmark recognition system can be implemented for other cities. As a future study, we plan to implement semantic segmentation architectures before the object recognition process as a tool for background elimination. Segmentation would prevent the learning of other objects that do not express the historic structure. Additionally, we plan to increase the number of recognizable historical buildings and to design our own deep learning architecture for historic landmark recognition purposes.

REFERENCES

- Amato, F., Moscato, V., Picariello, A., Colace, F., Santo, M.D., Schreiber, F.A., Tanca, L. (2017). Big data meets digital cultural heritage: Design and implementation of scrabs, a smart context-aware browsing assistant for cultural environments. *Journal on Computing and Cultural Heritage (JOCCH)*, 10 (1), 6.
- Brown, B. (2007). Working the problems of tourism. *Annals of Tourism Research*, 34 (2), 364-383.
- Cheng, Z., Shen, J. (2016). On very large scale test collection for landmark image search benchmarking. *Signal Processing*, 124, 13-26.
- Chollet, F. (2015). Keras: Deep learning for humans, Github. <https://github.com/keras-team/keras>
- CoreML Documentation, (2019). Converting Trained Models to Core ML, <https://developer.apple.com/documentation/core>

- ml/convertting_trained_models_to_core_ml [Accessed on 2 November 2019].
- CoreML Framework, (2019). CoreML Framework Overview, <https://developer.apple.com/documentation/coreml> [Accessed on 2 November 2019].
- Core Location Framework, (2019). Core Location Framework Overview, <https://developer.apple.com/documentation/corelocation> [Accessed on 2 November 2019].
- Deng, J., Berg, A., Satheesh, S., Su, H., Khosla, A., Fei-Fei, L. (2012). ImageNet Large Scale Visual Recognition Competition (ILSVRC2012). <http://www.image-net.org/challenges/LSVRC/2012/>.
- Doğan Y., Yakar, M. (2018). GIS and three-dimensional modeling for cultural heritages. *International Journal of Engineering and Geosciences*, 3 (2), 50–55.
- Gunawan, A.A., Surya, K., Meiliana. (2018). Brainwave classification of visual stimuli based on low cost EEG spectrogram using DenseNet. *Procedia Computer Science*, 135, 128–139.
- Hays, J., Efros, A.A. (2008). IM2GPS: Estimating geographic information from a single image. In *26th IEEE Conference on Computer Vision and Pattern Recognition (CVPR)*.
- He, K., Zhang, X., Ren, S., Sun, J. (2016a). Deep residual learning for image recognition. In *Proceedings of the IEEE conference on computer vision and pattern recognition*, pp. 770–778.
- He, K., Zhang, X., Ren, S., Sun, J. (2016b). Identity mappings in deep residual networks. In *Lecture Notes in Computer Science (Including Subseries Lecture Notes in Artificial Intelligence and Lecture Notes in Bioinformatics)*, pp. 630–645.
- Huang, C., Xu, H., Xie, L., Zhu, J., Xu, C., Tang, Y. (2018). Large-scale semantic web image retrieval using bimodal deep learning techniques. *Information Sciences*, 430–431, 331–348.
- Huang, F., Zhang, X., Zhao, Z., Li, Z., He, Y. (2018). Deep multi-view representation learning for social images. *Applied Soft Computing Journal*, 73, 106–118.
- Huang, G., Liu, Z., Van Der Maaten, L., Weinberger, K.Q. (2017). Densely connected convolutional networks. In *Proceedings - 30th IEEE Conference on Computer Vision and Pattern Recognition - CVPR 2017*, pp. 2261–2269.
- IPDCT - Istanbul Provincial Directorate of Culture and Tourism, (2019a). Where I am: Maiden's Tower, <http://www.istanbulkulturturizm.gov.tr/EN-171825/maidens-tower.html> [Accessed on 12 September 2019].
- IPDCT - Istanbul Provincial Directorate of Culture and Tourism, (2019b). Where I am: Sultanahmet Mosque (Blue Mosque), <http://www.istanbulkulturturizm.gov.tr/EN-174344/sultanahmet-mosque-blue-mosque.html> [Accessed on 12 September 2019].
- IPDCT - Istanbul Provincial Directorate of Culture and Tourism, (2019c). Where I am: Galata Tower, <http://www.istanbulkulturturizm.gov.tr/EN-171079/galata-tower.html> [Accessed on 12 September 2019].
- IPDCT - Istanbul Provincial Directorate of Culture and Tourism, (2019d). Where I am: Ayasofya Museum, <http://www.istanbulkulturturizm.gov.tr/EN-171028/ayasofya-museum.html> [Accessed on 12 September 2019].
- IPDCT - Istanbul Provincial Directorate of Culture and Tourism, (2019e). Where I am: Ortakoy Mosque, <http://www.istanbulkulturturizm.gov.tr/TR-209469/ortakoy-camii.html> [Accessed on 12 September 2019].
- IPDCT - Istanbul Provincial Directorate of Culture and Tourism, (2019f). Where I am: Topkapı Palace, <http://www.istanbulkulturturizm.gov.tr/EN-174359/topkapi-palace.html> [Accessed on 12 September 2019].
- IPDCT - Istanbul Provincial Directorate of Culture and Tourism, (2019g). Where I am: Dolmabahçe Palace, <http://www.istanbulkulturturizm.gov.tr/EN-171052/dolmabahce-palace.html> [Accessed on 12 September 2019].
- IPDCT - Istanbul Provincial Directorate of Culture and Tourism, (2019h). Where I am: Dikilitas (Theodosius Sütunu), <http://www.istanbulkulturturizm.gov.tr/TR-209450/dikilitas-theodosius-sutunu.html> [Accessed on 12 September 2019].
- IPDCT - Istanbul Provincial Directorate of Culture and Tourism, (2019i). Where I am: Dolmabahce Clock Tower, <http://www.istanbulkulturturizm.gov.tr/EN-171039/dolmabahce-clock-tower.html> [Accessed on 12 September 2019].
- Jiang, B., Yang, J., Lv, Z., Tian, K., Meng, Q., Yan, Y. (2017). Internet cross-media retrieval based on deep learning. *Journal of Visual Communication and Image Representation*, 48, 356–366.
- Keras Documentation, (2019). <https://keras.io/optimizers/> [Accessed on 25 August 2019].
- Lin, M., Chen, Q., Yan, S. (2013). Network in network. *arXiv preprint arXiv:1312.4400*.
- MapKit Framework, (2019). <https://developer.apple.com/documentation/mapkit> [Accessed on 12 September 2019].
- Maskrey M., Wang W. (2018). Using facial and text recognition. In *Pro iPhone Development with Swift 4*, pp. 285-315, Apress, Berkeley, CA.
- McGookin, D., Tahiroğlu, K., Vaitinen, T., Kytö, M., Monastero, B., Carlos Vasquez, J. (2019). Investigating tangential access for location-based digital cultural heritage applications. *International Journal of Human Computer Studies*, 122, 196–210.
- Mulazimoglu, E., Basaraner, M. (2019). User-centred design and evaluation of multimodal tourist maps. *International Journal of Engineering and Geosciences*, 4 (3), 115–128.
- Nawaz, M., Sewissy, A.A., Soliman, T.H.A. (2018). Multi-class breast cancer classification using deep learning convolutional neural network. *International Journal of Advanced Computer Science and Applications*, 9 (6), 316–332.
- Nibali, A., He, Z., Wollersheim, D. (2017). Pulmonary nodule classification with deep residual networks. *International Journal of Computer Assisted Radiology and Surgery*, 12 (10), 1799–1808.

- Parkhi, O.M., Vedaldi, A., Zisserman, A. (2015). Deep face recognition. In *Proceedings of the British Machine Vision Conference 2015*, pp. 41.1–41.12.
- Patterson J., Gibson A. (2017). Deep learning: A Practitioner's approach. *O'Reilly Media*, Sebastopol, CA, USA.
- Richards, G. (2018). Cultural tourism: A review of recent research and trends. *Journal of Hospitality and Tourism Management*, 36, 12–21.
- Rothe, R., Timofte, R., Van Gool, L. (2018). Deep expectation of real and apparent age from a single image without facial landmarks. *International Journal of Computer Vision*, 126 (2–4), 144–157.
- Schaul, T., Antonoglou, I., Silver, D. (2014). Unit tests for stochastic optimization. In *International Conference on Learning Representations*. arXiv:1312.6055.
- Shukla, P., Rautelai, B., Mittal, A. (2017). A computer vision framework for automatic description of Indian monuments. In *13th International Conference on Signal-Image Technology & Internet-Based Systems (SITIS)*, 4–7 December, Jaipur, India.
- Simonyan, K., Zisserman, A. (2014). Very deep convolutional networks for large-scale image recognition. *arXiv preprint arXiv:1409.1556*.
- Soon, F. C., Khaw, H.Y., Chuah, J.H., Kanesan, J. (2018). Hyper-parameters optimisation of deep CNN architecture for vehicle logo recognition. *IET Intelligent Transport Systems*, 12 (8), 939–946.
- Şasi A., Yakar, M. (2018). Photogrammetric modelling of Hasbey Dar'ülhuffaz (Masjîd) using an unmanned aerial vehicle. *International Journal of Engineering and Geosciences*, 3 (1), 6–11.
- Termritthikun, C., Kanprachar, S., Muneesawang, P. (2018). NU-LiteNet: Mobile landmark recognition using convolutional neural networks. *arXiv preprint arXiv:1810.01074v1*.
- Tzelepi, M., Tefas, A. (2018). Deep convolutional image retrieval: A general framework. *Signal Processing: Image Communication*, 63, 30–43.
- UNESCO, (2006). Cities Named '2010 European Capital of Culture' include World Heritage sites. <https://whc.unesco.org/en/news/248/> [Accessed on 12 September 2019].
- Weyand, T., Leibe, B. (2015). Visual landmark recognition from Internet photo collections: A large-scale evaluation. *Computer Vision and Image Understanding*, 135, 1–15.
- Xu, H., Huang, C., Wang, D. (2019). Enhancing semantic image retrieval with limited labeled examples via deep learning. *Knowledge-Based Systems*, 163, 252–266.
- Yorulmaz M., Celik, O.C. (1995). Structural analysis of the Bozdoğan (Valens) aqueduct in Istanbul. In *Arch Bridges, Ed. C.Melbourne, Thomas Telford*, London, 175–180.
- Zeiler, M.D. (2012). ADADELTA: an adaptive learning rate method. *arXiv preprint arXiv:1212.5701*.
- Zhang, D., Han, X., Deng, C. (2018). Review on the research and practice of deep learning and reinforcement learning in smart grids. *CSEE Journal of Power and Energy Systems*, 4 (3), 362–370.
- Zhou, B., Lapedriza, A., Khosla, A., Oliva, A., Torralba, A. (2018). Places: A 10 million image database for scene recognition. *IEEE Transactions on Pattern Analysis and Machine Intelligence*, 40 (6), 1452–1464.
- URL1:
<https://github.com/fchollet/deep-learning-models> [Accessed 10 September 2019]
- URL2:
<https://github.com/raghakot/keras-resnet> [Accessed 10 September 2019]
- URL3:
<https://github.com/flyyufelix/DenseNet-Keras> [Accessed 10 September 2019]



© Author(s) 2020. This work is distributed under <https://creativecommons.org/licenses/by-sa/4.0/>



Mersin Photogrammetry Journal

<https://dergipark.org.tr/tr/pub/mephoj>

e-ISSN 2687-654X



Comparison of documentation cultural artifacts using the 3D model in different software

Abdurahman Yasin Yiğit ¹, Yunus Kaya ², Adem Kabadayı ³

¹Mersin University, Faculty of Engineering, Geomatics Engineering, Mersin, Turkey

²Harran University, Faculty of Engineering, Geomatics Engineering, Şanlıurfa, Turkey

³Yozgat Bozok University, Şefaati Vocational High School, Department of Architecture and Urban Planning, Yozgat, Turkey

Keywords

Close-range Photogrammetry
Documentation
UAV
3D model
Different Software

ABSTRACT

The creation and drawing of a three-dimensional (3D) model of historical and cultural buildings have become an important issue. Especially in terms of protecting these historical buildings and transferring future generations, their importance is gradually increasing. Close-range photogrammetry is a method used for many years. With the development of computer and information technology, the classical close-range photogrammetry method has been replaced by the digital close-range photogrammetry method. Digital photogrammetry methods are easier to perform with a computer than conventional methods. By close-range photogrammetry method; it can offer many products such as orthophoto, 3D model, drawing, digital surface, and terrain. In this study, photogrammetric research was carried out for documentation purposes in Cimcime Hatun Tomb in Erzurum. In the study, the hybrid method was applied by taking photos from the unmanned aerial vehicles (UAV) and ground. The 3D model study was carried out in 3 different software (Agisoft PhotoScan, Context Capture, Photomodeler UAS). At the end of the study, the advantages and disadvantages of this software have been discussed. As a result of the study, the position accuracy (X, Y, Z) of Agisoft Photoscan, Context Capture, and Photomodeler UAS software was calculated as 2.17, 2.73, 1.73 cm.

1. INTRODUCTION

Cultural heritages not only ensure the continuity of the experiences and traditions that people have accumulated throughout history but also ensure the correct planning of the future. In addition, societies, they see their cultural heritage as defining elements of their national identity. The protection of such important monuments is regarded as equivalent to the protection of national identities. In fact, societies have embarked on scientific research activities on the origin of these elements to embrace these values as their cultural heritage. Because it enables us to increase the studies in this field and thus to reveal those who are forgotten from these values. In this context, the importance of preserving and documenting cultural heritage works has been the subject of research by different disciplines.

One of the important steps to protect historical artifacts is to make the documentation accurate and precise. Modern and technological documentation methods: It is preferred more in terms of time and cost

than traditional methods in determining deformations, measuring and drawing historical buildings, and preparing restoration projects. With the effective use of technology in this area, new perspectives have been introduced to the documentation methods. Especially in digital platforms, the use of 3D model documentation methods has increased. Different methods are used for documentation with the 3D model. Among these methods, especially the contactless data collection strategy with the photogrammetry method come to the fore.

Photogrammetry is used effectively in the documentation of cultural heritage to produce 3D models of historical buildings and artifacts (Uslu and Uysal, 2017; Uslu et. al, 2016; Zeybek and Kaya, 2020).

Yakar et al. (2018) investigated the photogrammetric method and the usability of GIS to document cultural heritage. In the study, the 3D model of a cultural structure was obtained from the images obtained by close-range photogrammetry.

* Corresponding Author

*(ayasinyigit@mersin.edu.tr) ORCID ID 0000-0002-9407-8022
(yunuskaya@harran.edu.tr) ORCID ID 0000-0003-2319-4998
(ademkabadayi@gmail.com) ORCID ID 0000-0002-4891-8131

Cite this study

Yiğit A Y, Kaya Y & Kabadayı A (2020). Comparison of documentation cultural artifacts using the 3D model in different software. Mersin Photogrammetry Journal, 2(2), 51-58

Ulvi and Toprak (2016) in their work, have touched upon the use of very different techniques in cultural heritage documentation. They mentioned that one of these methods is the close-range photogrammetry technique. They created a 3D model using this technique. At the end of the study, they documented the historical artifact on the digital platform. They mentioned that this model can be used as a base for restoration work that can be done later. They suggested that numerical data can be used by creating a tourism information system in order to introduce the artifact in terms of tourism.

Şasi and Yakar (2017) used the close-range photogrammetry technique in their documentation study. They mentioned that close-range photogrammetry was insufficient in some works within the scope of this study. They pointed out that the roofs of the buildings are missing especially in the photographs taken from the ground and that the 3D model cannot be created with exactly the required precision. They mentioned the importance of using unmanned aerial vehicles (UAVs) in eliminating this shortcoming.

The same problem was encountered in this study as stated in the documentation studies made with the close-range photogrammetry method. That's why in the study, photographs were taken both from the unmanned aerial vehicle (UAV) and from the ground. The use of UAV in documenting cultural heritage in this way is gaining importance day by day. Especially UAVs, it facilitated photographing and documenting the inaccessible parts of the structures. With the use of UAVs in different studies effectively, the definition of UAV photogrammetry has emerged in the literature.

In 3D documentation studies using the photogrammetry technique, point position accuracy is usually investigated through a single software. In this study, the point position accuracy of different software has been investigated (Ulvi et al., 2019; Yakar et al., 2016). Also, the 3D model study was carried out in 3 different software (Agisoft PhotoScan, Context Capture, Photomodeler UAS). At the end of the study, the advantages and disadvantages of this software have been discussed.

2. MATERIAL and METHOD

The study was carried out in 2 stages: A field study and office work.

In fieldwork, image data is collected, and precise measurements were made. The images were collected from two different way, aerial, and ground.

Images taken from the ground were taken with the Nikon D3100 camera shown in Figure 1. The technical specifications of the camera are given in Table 1.



Figure 1. Nikon D3100 camera

Table 1. Nikon D3100 camera specification (URL-1)

Specification	Value
Megapixels	14.20 MP
Sensor	23.1 x 15.4 mm
Sensor resolution	4616 x 3077
Sensor size	23.1 x 15.4 mm
Surface area	355.7 mm ² mm
Pixel pitch & Pixel area	5 µm & 25 µm

Aerial images were taken with the Phantom 3 Pro UAV shown in Figure 2. The technical features of Phantom 3 Pro UAV are shown in Table 2.



Figure 2. Phantom 3 Pro UAV (URL-2)

Table 2. Phantom Pro 3 specification (URL-2)

Specification	Value
Weight & Diagonal Size	1280 g & 350 mm
Max Ascent & Descent Speed	5 m/s & 3 m/s
Max Speed	16 m/s (ATTI mode)
Max Tilt Angle	35°
Max Flight Time	Approx. 23 minutes
Satellite Positioning Systems	GPS/GLONASS
Sensor & Lens	1/2.3" & 20mm

In the study, the photogrammetry was used as a method.

Photogrammetry generally deals with the mathematical representation of the geometrical relations between physical objects in three-dimensional space based on their images recorded on a two-dimensional space. Over the years, photogrammetry has been used routinely in aerial photogrammetry, cartography, documentation, and remote sensing (Wolf, 1974; Ulvi, 2008).

In photogrammetry, images obtained by numerically recording electromagnetic rays reflected from objects are evaluated. It can be described as the technique of obtaining information about objects without direct contact with objects (Grussenmeyer et al., 2008; McCarthy, 2014).

The images contain all the data about the object. From these data, photogrammetric evaluation can be conducted at any time. For this reason, these images were used to document important works. Photogrammetry, which is used as a method of processing these data, is frequently preferred.

In this study, 3 different photogrammetry software (Agisoft PhotoScan, Context Capture, Photomodeler UAS) is used to obtain a 3D model from 2D images and the position accuracy of the points was calculated according to equation 1,2 and 3.

$$SXO = \sqrt{\frac{V_x V_x}{n-1}} \tag{1}$$

$$SYO = \sqrt{\frac{V_y V_y}{n-1}} \tag{2}$$

$$SZO = \sqrt{\frac{V_z V_z}{n-1}} \tag{3}$$

3. APPLICATION

3.1. Study Area

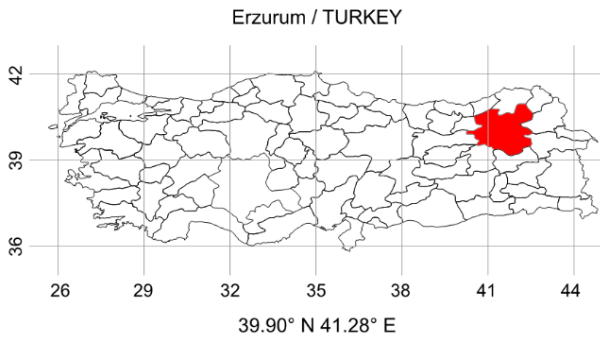


Figure 3. Erzurum location

The tomb known as Cimcime Sultan Tomb has located the Erzurum city of Turkey (Figure 3). The tomb was built in the 14th century (URL-3). The grave is in the shape of a cylinder with a conical roof. Twelve blind arches, consisting of a continuous pattern, decorate the edges of the tomb (Figure 4). The tomb is located at the latitude of 39.906257° N and the longitude of 41.276784° E.



Figure 4. General view of the tomb

3.2. Creation the 3D Model

Images were taken in different angles and distances to cover the entire object. When taking images, care was taken to the angle of arrival of the sun. Also, no contact was made to avoid damaging the object. 25 of the Tomb's specific points were measured by using Total station. 13 of them were used for orientation. 12 of them were used as checkpoints (CHP).

After the field work was completed, the 3D model was created various in the photogrammetric software. 3 different software were compared with 12 control points. 3 different software were compared with 12 CHPs. In the study, 25 UAV images and 38 ground images were used.

3.2.1. Agisoft PhotoScan Software

This software was chosen because it is the most used software in the literature. The software offers low cost and it is simple to use. It is also preferred because it contains SfM algorithms (Ulvi et al., 2020).

Camera calibration was done automatically in Agisoft software.

In the 3D model, firstly the process of "tie" and "orientation" the images with each other was executed (Align process) (Figure 5). After the "tie point" was produced, a "dense point cloud" was created (Figure 6). Last, the "mesh" and the "3D model" was produced (Figure 7).



Figure 5. Tie point (49,468) in Agisoft PhotoScan

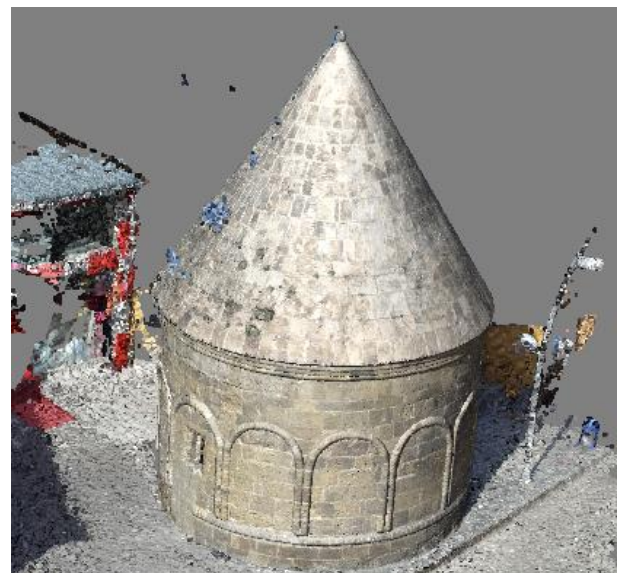


Figure 6. Dense cloud point in Agisoft PhotoScan (13,247,333)

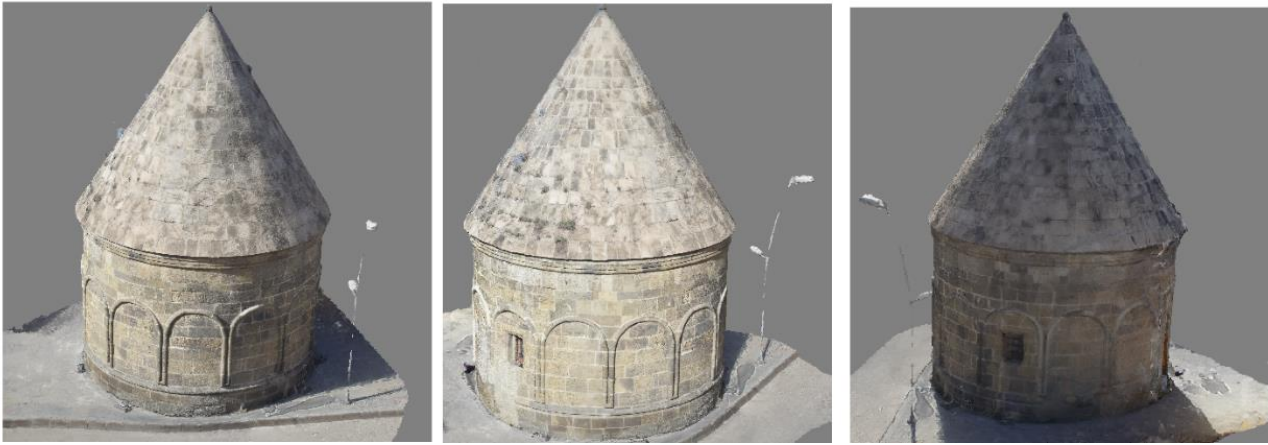


Figure 7. 3D model in Agisoft PhotScan

3.2.2. Context Capture Software

This software has been preferred because it is used less in the literature. It is more expensive than other software. But it is simple to use. Agisoft software needs to create a dense point cloud for the 3D model. Context Capture does not need a dense point cloud to create 3D models it is optional. Firstly, the tie point is created from the images and oriented (Aerotriangulation).

The created tie point is shown in figure 8. The dense cloud and 3D model are shown in Figures 9 and 10, respectively.

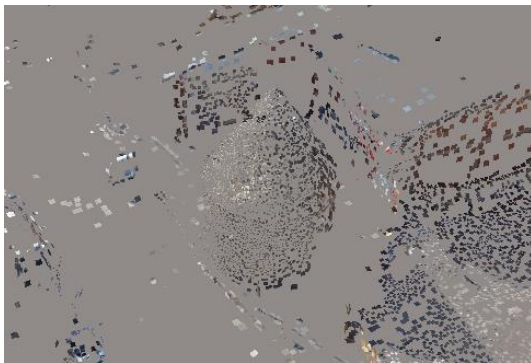


Figure 8. Tie point in Context Capture (20,919)



Figure 9. Dense cloud point Context Capture (173,407,269)



Figure 10. 3D model in Context Capture

3.2.3. Photomodeler UAS Software

This software is preferred because it has the feature of drawing. Due to this feature, it provides additional advantage compared to other 3D model software. It is difficult to use compared to other software.

Camera calibration is performed first in Photomodeler UAS software.

Accurate calibration parameters increase the accuracy of the orientate process. Orientation is more impeccable thanks to the beams coming from different angles and distances. For this purpose, the calibration process was performed in the study.

The template shown in Figure 11 was used for calibration.

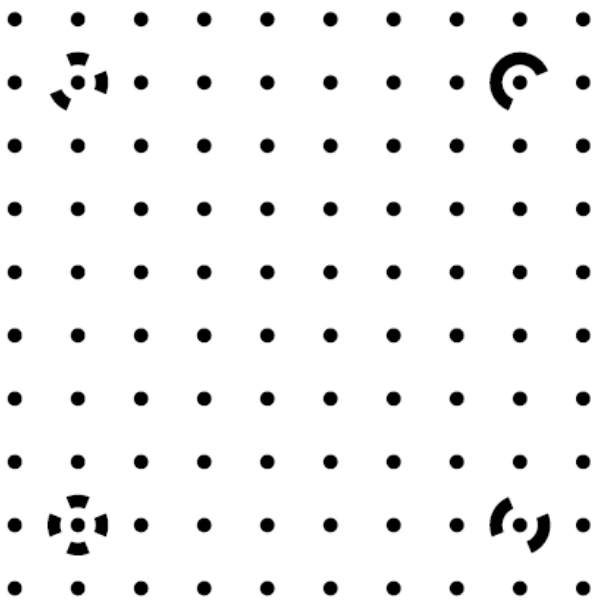


Figure 11. Calibration Paper

Figure 12 shows the calibration process performed in the software.

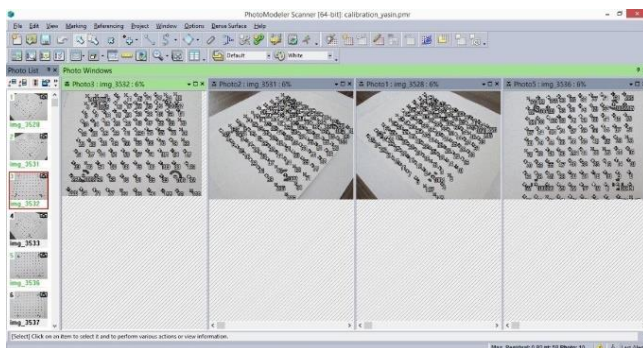


Figure 12. Create the calibration parameters

After the calibration process was completed, orientation was performed (Figure 13).

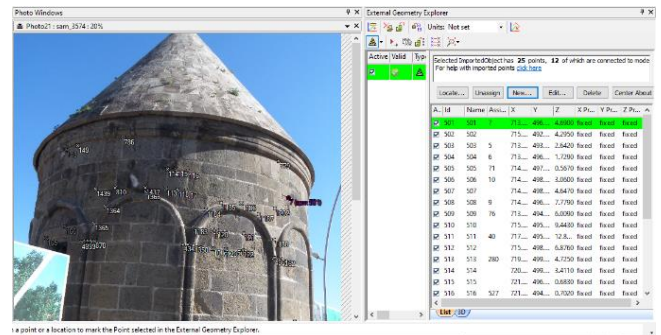


Figure 13. Oriented process

Drawings were made after the orientation process (Figure 14).

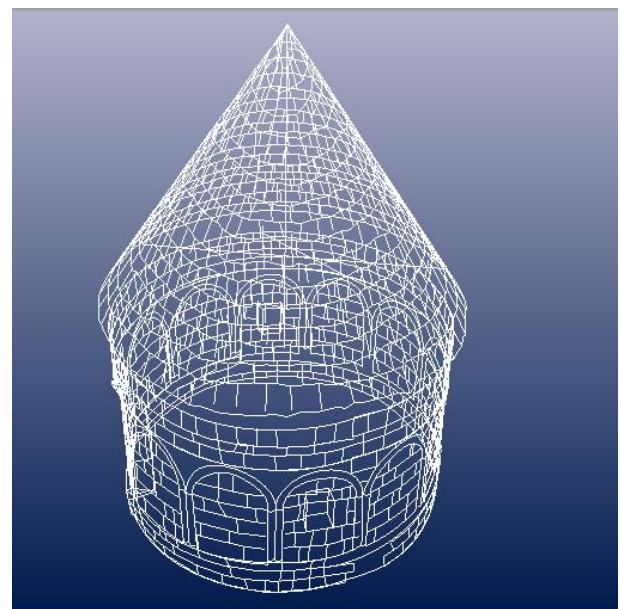


Figure 14. Drawing process and 3D model

During the drawing process, 1112 lines and 220 curve lines were used.

After drawing, the surface was created, and the 3D model was obtained.

After drawing, the surface was created, and the 3D model was obtained. The surfaces are covered by specifying the lines drawn in the Photomodeler UAS software. The lines covered with the surface are passed through the actual texture with appropriate images (Figure 15). At the end of the study, CHPs were compared in all 3 software (Table 3).



Figure 15. 3D model in Photomodeler UAS

Table 3. Comparison of CHPs

N.N.	Survey Coordinates			Agisoft Photoscan			Context Capture			Photomodeler		
	X (m)	Y (m)	Z (m)	Vx(cm)	Vy(cm)	Vz(cm)	Vx(cm)	Vy(cm)	Vz(cm)	Vx(cm)	Vy(cm)	Vz(cm)
501	496.137	713.669	4.690	1.6	0.9	-2.0	2.2	1.5	-0.6	0.4	0.7	-1.0
502	492.403	715.039	4.295	0.6	1.2	-2.4	1.2	2.0	-1.4	0.6	0.4	-0.8
503	496.028	713.628	1.729	-1.6	0.7	1.3	-1.8	1.7	1.7	-1.4	0.8	0.5
504	498.15	714.534	3.060	-1.1	-2.0	0.9	-1.8	-1.5	1.5	-0.9	-1.1	1.2
505	498.261	714.598	4.647	0.7	-0.6	-1.7	1.3	-1.2	-1.5	0.9	-0.9	-0.8
506	494.845	713.438	6.009	0.7	-1.4	1.4	1.4	-1.8	1.8	0.2	-1.0	1.5
507	499.476	719.23	4.725	0.3	1.1	1.8	-0.8	2.0	1.6	-1.2	1.1	1.8
508	495.591	717.788	8.861	-0.8	0.8	-1.0	-1.7	1.4	-1.8	-2.9	1.0	-1.2
509	496.027	721.901	0.683	1.4	-1.2	-1.4	2.0	-1.7	-1.6	0.4	-0.5	-1.3
510	495.439	721.896	3.669	0.2	-1.1	0.7	2.0	-1.5	1.9	-0.3	-1.2	0.9
511	493.04	721.275	4.122	0.9	1.6	-1.3	1.7	1.4	-0.4	1.0	-0.8	0.7
512	495.968	721.998	6.517	1.5	-0.8	0.8	1.3	-1.7	0.4	0.5	-0.1	0.1
				mxyz= 2.17			mxyz= 2.73			mxyz= 1.79		

4. CONCLUSIONS and DISCUSSION

All software used in the study (Agisoft PhotoScan, Context Capture, Photomodeler UAS) are frequently used in documentation studies with photogrammetric techniques. Agisoft PhotoScan software is the most preferred software. Because it has easy usage. Although Context Capture software

is easy to use, it is not preferred frequently. Because it is expensive. Photomodeler UAS software is difficult to use. But it is preferred because of its drawing ability. The general assessment of the software is shown in table 4.

Table 4. The general assessment of the software

Software	Calibration	Orientation	Point Cloud	Mesh	Draw	3D Model	Usage	Price
Agisoft PhotoScan	Semi automatic Automatic	Easy	Required Medium (13,247,333) Optional	Good	Yes (Weak)	Easy Good	Easy	Cheap
Context Capture	Automatic	Average	Dense (173,407,269)	Best	No	Easy Good	Easy	Expensive
Photomodeler UAS	Manuel Semi automatic Automatic	Hard	Optional (Not Produced)	Medium	Yes (Strong)	Hard Medium	Hard	Cheap

When table 4 is examined, there are advantages and disadvantages to all software.

Calibration: Calibration is the first step of the photogrammetric process. Calibration is executed automatically in Context Capture software. In the Agisoft PhotoScan software, calibration is done semi-and fully automatically. In other words, parameters can be entered

both by the operator and created by the software. In Photomodeler UAS software, the calibration process can be defined manually, unlike other software. These parameters can be determined using a calibration paper. This provides convenience to the operator, especially in the orientation process.

Orientation: Orientation is the process of determining the position and orientation of two images in three-dimensional space. In Agisoft PhotoScan software, the images are aligned before orientation. Aligned images are completed in a fully automated using the Sfm (structure from motion) method. Manual tie points can be used if needed. Although the process is carried out fully automatically in Context Capture software, since it uses "aerotriangulation" as the basic algorithm, it is not as optimum as the Sfm method. In the situation, there is a problem in orientation the images taken from different distances. Although the process can be executed automatically in Photomodeler UAS software, the expected result cannot be acquired. So, it is more suitable to manually match the images one by one. This situation causes both a take long time and the difficulty of the process.

Point Cloud: Creating the dense point cloud in Photomodeler software is optional. This stage has not been done since the Photomodeler UAS software could not produce the expected accuracy from the point cloud. Creating the dense point cloud in Context Capture software is optional. Generally, in Context Capture software, the 3D model is produced without generating a point cloud. This is because the point cloud produced in the software is very dense. This causes the computer central processing unit (CPU) to run slowly. It is required to generate a point cloud in order to produce a 3D model in Agisoft PhotoScan software. The process takes place fully automatically. It produces sparse point clouds according to Context Capture software.

Draw: In Agisoft PhotoScan software, drawing is used only for determining straight lines. The drawing of complex lines is not at the expected level. In the Photomodeler software, complex lines can be drawn. At least two different images are required to draw a line. To increase the accuracy of the drawn line, the number of images should be increased. Every line drawn must be reorientated. This situation causes the process to be both difficult and takes a long time.

Mesh and 3D Model: The quality of mesh in Photomodeler UAS software depends on the accuracy of the lines drawn. Mesh cannot be created because some lines cannot be drawn. This results in a low-quality Mesh and 3D model. Mesh quality in Agisoft PhotoScan software depends on the point cloud. The denser point cloud is produced, the better-quality Mesh and 3D model is produced. Structures with complex and many recesses are difficult to model. Context Capture software uses a very dense matching method. Therefore, the mesh and 3D models produced are of high quality. When the figures 7 and 10 are examined, the difference between the lighting post and the curves can be observed.

Usage: In Agisoft PhotoScan and Context Capture software, only CHPs are marked manually. It is easy to usage as all the other processes are fully automated. In Photomodeler UAS software, most of the process is done manually by the operator. Especially the orientation and drawing processes are difficult and take a long time. Many problems are encountered because it depends on the operator. So, it is difficult to usage.

In summary, every software has its advantages and disadvantages. It is necessary to choose the appropriate

software according to the project. Therefore, good research about the software is required before starting to work.

5. RESULT

The photogrammetry method by different disciplines is frequently preferred in documentation studies. In the photogrammetry method, the images of all facades of the work cannot be taken completely. In 3D documentation of the cultural heritage, images that will see all the facades of the work are needed. All the facades of the work should be photographed to meet this need. The images of the facades which are not visible in the images taken from the ground must be taken in different locations. Especially the images of the upper facades should be taken from the air. It can be easily realized with the UAV carrier platforms that have been used for this purpose recently for the aerial images.

Images taken from both different locations were processed in photogrammetric software and a 3D model was created. In this study three different software is used for the 3D model. They are basically based on the same working principle. Some processes followed by software make a difference.

The Agisoft Photoscan software used in the study consists of 4 main processes. These are "align", "dense cloud", "mesh", and "texture", respectively. The Context Capture software used in the study consists of 2 main processes. These are "aerotriangulation", and "mesh", respectively. If desired "dense cloud" can be created in Context Capture software. The Photomodeler UAS software used in the study consists of 4 main processes. These are "calibration", "orientation", "draw", and "texture" respectively.

Tie point and dense cloud are creating in both Agisoft PhotoScan and Context Capture software. When these products are compared, for tie point: in Agisoft PhotoScan software created 49 468 and in Context Capture software created 20 919. For the dense cloud: in Agisoft PhotoScan software created 13 247 333 and in Context Capture software created 173 407 269.

When all processes of photogrammetry were examined, it took approximately 120, 100, 300 minutes respectively in Agisoft Photoscan, Context Capture, and Photomodeler UAS software.

When the orientation result was examined, the position accuracy (X, Y, Z) 2.17, 2.73, 1.73 cm were calculated in Agisoft Photoscan, Context Capture, and Photomodeler UAS software, respectively.

At the end of the study, the 3D model and documentation of the historical Tomb were made on the digital platform. In the study, both close-range and UAV photogrammetry methods were applied as hybrid methods. The integration of the photos collected by both methods has been successfully completed. As a result, these two methods are complementary methods rather than alternative methods. Both UAV and close-range photogrammetry should be used to document complex structures with the photogrammetry method. Appropriate software should be selected according to the project. The point position accuracy of 3 different software used in the study is close to each other. All

three-software used in the study can be used in 3D documentation studies.

REFERENCES

- GRUSSENMEYER, P., LANDES, T., VOEGTLE, T. & RINGLE K. (2008). Comparison Methods of Terrestrial Laser Scanning, Photogrammetry and Tacheometry Data for Recording of Cultural Heritage Buildings. *The International Archives of the Photogrammetry, Remote Sensing and Spatial Information Sciences*, 37.
- McCARTHY, J. (2014). Multi-image Photogrammetry as a Practical Tool for Cultural Heritage Survey and Community Engagement. *Journal of Archaeological Science*, 43, 175-185.
- ŞASI, A., & YAKAR, M. (2017). Photogrammetric Modelling of Hasbey Dar'ülhuffaz (Masjid) Using an Unmanned Aerial Vehicle. *International Journal of Engineering and Geosciences*, 3(1), 6-11.
- ULVİ, A. (2008). Antik Tiyatroların Fotogrametrik Rölöve Planlarının Çıkarılması Üzerine Deneysel Bir Çalışma. *Selçuk Üniversitesi Fen Bilimleri Enstitüsü, Fotogrametri Anabilim Dalı, Yüksek Lisans Tezi*, 2008.
- ULVİ, A., & TOPRAK, A.S. (2016). Investigation of Three-Dimensional Modelling Availability Taken Photograph of the Unmanned Aerial Vehicle; Sample of Kanlıdivane Church. *International Journal of Engineering and Geosciences*, 1(1), 1-7.
- Ulvi, A., Yakar, M., Yiğit, A. & Kaya, Y. (2019). The Use of Photogrammetric Techniques in Documenting Cultural Heritage: The Example of Aksaray Selime Sultan Tomb. *Universal Journal Of Engineering Science*, 7(3), 64-73.
- Ulvi, A., Yakar, M., YİĞİT, A. Y., & Kaya, Y. (2020). İHA ve Yersel Fotogrametrik Teknikler Kullanarak Aksaray Kızıl Kilise'nin 3 Boyutlu Nokta Bulutu ve Modelinin Üretilmesi. *Geomatik Dergisi*, 5(1), 22-30.
- USLU, A., & UYSAL, M. (2017). Arkeolojik Eserlerin Fotogrametri Yöntemi ile 3 Boyutlu Modellenmesi: Demeter Heykeli Örneği. *Geomatik Dergisi*, 2 (2), 60-65.
- USLU, A., POLAT, N., TOPRAK, A.S., & UYSAL, M. (2016). Kültürel Mirasın Fotogrametrik Yöntemle 3B Modellenmesi Örneği. *Electronic Journal of Map Technologies*, 8(2), 165-176.
- WOLF, P. R. (1974), Elements of Photogrammetry. New York: McGraw-Hill.
- Yakar, M., Kabadayı, A., Yiğit, A. Y., Çıkıkcı, K., Kaya, Y. & Catin, S. S. (2016). Emir Saltuk Kümbeti Fotogrametrik Rölöve Çalışması ve 3Boyutlu Modellenmesi. *Geomatik Dergisi*, 1(1), 14-18.
- Yakar, M., Orhan, O., Ulvi, A., Yiğit, A. Y. & Yüzer, M. M. (2015). Sahip Ata Külliyesi Rölöve Örneği. TMMOB Harita ve Kadastro Mühendisleri Odası, 10.
- ZEYBEK, M. & KAYA, A. (2020). Tarihi Yığma Kiliselerde Hasarların Fotogrametrik Ölçme Tekniğiyle İncelenmesi: Artvin Tbeti Kilisesi Örneği. *Geomatik*, 5 (1), 47-57.
- URL-1.
https://www.digicamdb.com/specs/nikon_d3100/
Retrieved: 08.04.2020
- URL-2.
<https://www.dji.com/phantom-3-pro/info>
Retrieved: 08.04.2020
- URL-3.
<https://archnet.org/sites/18000>
Retrieved: 31.05.2020



© Author(s) 2020. This work is distributed under <https://creativecommons.org/licenses/by-sa/4.0/>



Mersin Photogrammetry Journal

<https://dergipark.org.tr/tr/pub/mephoj>

e-ISSN 2687-654X



Determination of pond volume with using an unmanned aerial vehicle

Aydın Alptekin^{*1}, Murat Yakar²

¹Mersin University, Engineering Faculty, Geological Engineering Department, Mersin, Turkey

²Mersin University, Engineering Faculty, Geomatics Engineering Department, Mersin, Turkey

Keywords

Pond volume
UAV
3D model
DSM
Orthophoto

ABSTRACT

Water management will become a very important topic in the near future. Water scarcity has been seen in most of the world due to drought because of global warming. Water storage is paramount under water scarce situations. Mersin, characterized by the Mediterranean climate, has been negatively affected by climate change. Water retaining structures are needed to build to carry on agricultural activities all year round in the city. Advances in unmanned aerial vehicle (UAV) technologies have made it easier to model engineering projects. In this study, we modelled a site on which a pond will be built in the near future using a UAV. We created the Digital Surface Model (DSM) and orthophoto of the study area to measure the pond's volume and 3D surface area. The pond will become an economic component of the region.

1. INTRODUCTION

Unmanned aerial vehicle (UAV) can be used to model the terrain in very high resolution and accuracy with the help of Global Navigation Satellite System (GNSS). UAV has been frequently used in engineering projects since last decade. Rockfall simulation (Sarro et al. 2018), flood site modelling (Annis et al. 2020), landslide monitoring (Eker et al. 2017), damage caused by earthquake (Dominici et al. 2017), cultural heritage modelling (Şasi and Yakar 2018; Ulvi et. al 2020) are some of the studies that can be performed by using UAV.

Drought, which is a nature produced temporary imbalance of water availability (Pereira et al. 2002) is a serious threat to Turkey. Land surface temperature, which is very important to model the climate change and weather forecast (Orhan et al. 2019), increases each year in Konya, Turkey (Orhan and Yakar, 2016). Precipitation regime has been continuously changing due to global warming. This situation increases the necessity to build water retention structures. Ponds, which are generally used in agricultural activities, can store the dead loss surface water. The increased risk of drought increases the need for ponds. Management of water resources will become the main topic in near future.

We need a Drought Management Plan to increase the efficiency of irrigation system performance. Storage of water is one of the main items in this plan. Ponds are productive investments on agricultural activities.

In Turkey, studies about ponds have increased recently. Demirkıran et al. 2018 have measured dead volume of a pond with bathymetric methods. Keskiner et al. 2020 have created surface runoff models and determined pond volume by using geostatistical models. Akyıldız et al. 2020 have analyzed the use of waste materials of marble quarry as a filling material in a pond construction.

Water scarcity is a significant problem in most Eastern and Southern Mediterranean countries due to economic growth and inefficient usage in agricultural activities (Harmancıoğlu et al. 2008). The clean fresh water scarcity has to be considered with the physical shortage of water (Jia et al. 2020). Global climate change has negatively affected Turkey. Orhan et al. 2017 has investigated the water surface area in Salt Lake by using satellite images, and concluded that meteorological events caused the decrease in the lake area.

To improve water usage efficiency, water retaining structure needs to be constructed. In the design of a water structure, volume and 3D area have to be calculated. Any object that has irregular geometric shape needs to be gridded.

* Corresponding Author

(aydinalptekin@mersin.edu.tr) ORCID ID 0000 – 0002 – 5605 – 0758
(myakar@mersin.edu.tr) ORCID ID 0000 – 0002 – 2664 – 6251

Cite this article

Alptekin A & Yakar M (2020). Determination of pond volume with using an unmanned aerial vehicle. Mersin Photogrammetry Journal, 2(2), 59-63

To model a pond site completely, meteorological, morphological and geological factors of the terrain have to be considered. In addition to these, water balance components, anthropogenic activities, industrial demand and excessive usage is necessary (Swain et al. 2020).

Mersin has fertile farmland. With the increasing in industrial demand, agricultural activities will be an important component of the economic development of the region. Kerimler pond, which will be used for agricultural purposes, will be constructed in near future. In this study, we measured 3D area and volume of the pond site to determine the amount of membrane to be used to prevent leakage.

2. STUDY AREA

Agriculture and tourism are the main income in the region, characterized by Mediterranean climate. There are 55 large and small rivers (Bilici and Everest, 2017) in Mersin, all of which take their source from the Taurus Mountains. Study area is located in Kerimler Village, Mersin (Figure 1). Bahçepınarı groundwater source is located in Kerimler (MÇŞİM, 2018). Mersin, which has very fruitful farmland, has high precipitation rate in summer. Kerimler village got 972.26 mm average yearly rainfall in last 5 years (Figure 2). In 2019, average amount of rainfall is 98.89 mm monthly (Figure 3).

Fujihara et al. 2008 have modelled water usage in Seyhan River Basin, very close to Kerimler village. They concluded that impacts of climate change may decrease available water resources in the basin.

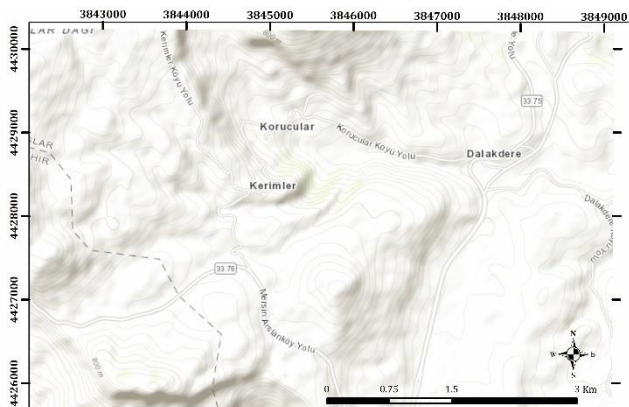


Figure 1. Location map of the study area

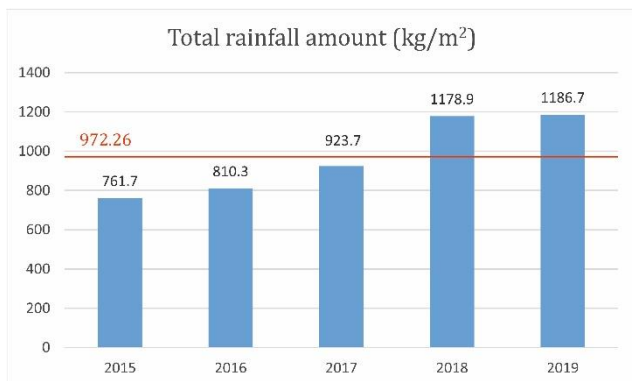


Figure 2. Total amount of rainfall in last 5 years

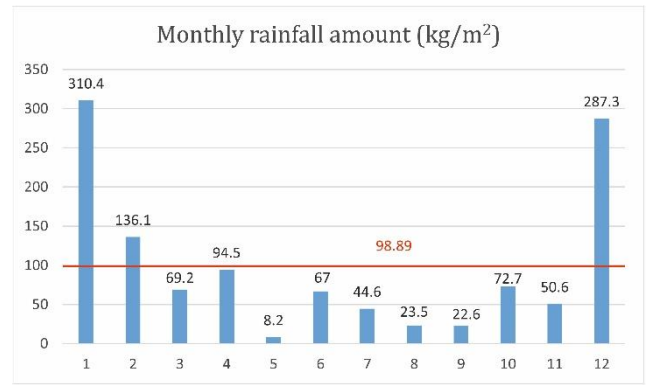


Figure 3. Monthly rainfall amount in 2019

The study area is located in between right-lateral (dextral) Kırkkavak fault and left-lateral (sinistral) Ecemiş Fault. Geyik Dağı, Aladağ, Bolkar Dağı, Bozkır, Antalya and Alanya units are the major tectono-stratigraphic units giving the complex nappe structure in Central Taurides (Özgül, 1983). Lower-Middle Miocene aged Karaisalı formation consists of limestone, is seen in Kerimler village (Figure 3).

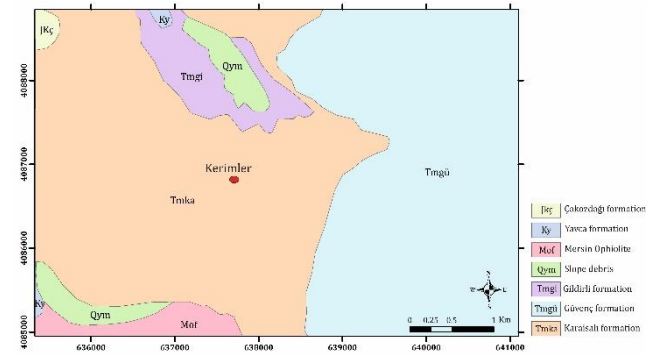


Figure 4. Geological map of the study area (Simplified from MTA, 2009)

3. METHOD

Photogrammetric methods allow users to create 3D model of the objects with higher accuracy (Ulvi and Yiğit 2019). Modeling the terrain in 3D with using a UAV has solved many engineering problems. Ulvi 2018 has measured the volume terrain by using a UAV. Kaya et al. 2019 have measured the volume of pond.

In this study, we used Anafi Parrot (Figure 5) to take pictures of the study area. Flight plan (Table 1) was prepared in Pix4Dcapture mobile application. In the study area, seven Ground control points (GCP) were determined homogenously to georeference the area (Figure 6).

Structure from motion (SfM) is the most preferred technique to create 3D model of the object from 2D pictures, which were taken with high overlap ratio.

There are many commercial software, which can model the terrain using pictures taken with UAV. Agisoft Metashape, which is user-friendly software, was used in this study.

Table 1. Flight plan

Property	Value
Flight height	47 m
GSD	1.57 cm/px
Overlay ratio	80%
Angle	90°
Flight time	6 min 52s



Figure 5. Anafi Parrot

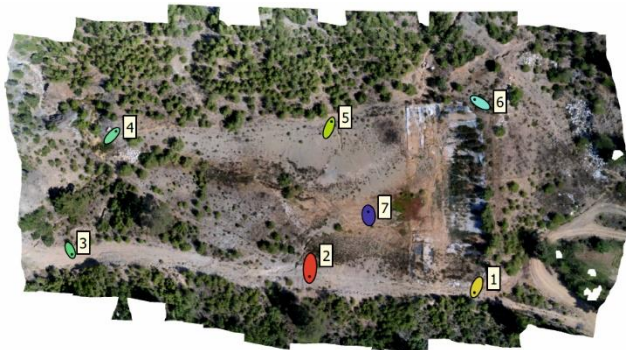


Figure 6. Ground control points

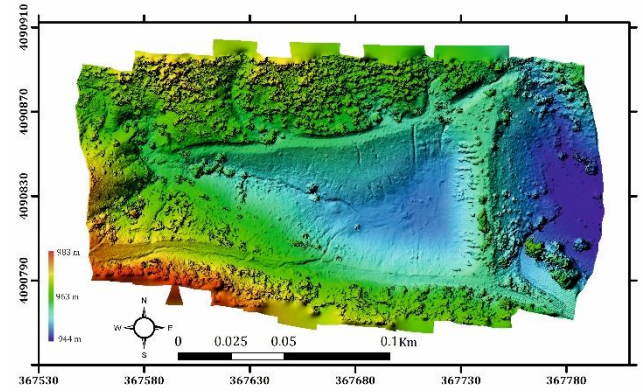


Figure 6. DSM

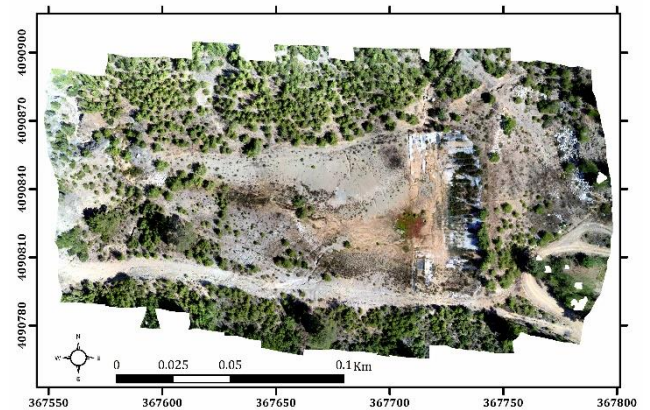


Figure 7. Orthophoto

4. RESULTS

Modelling the project was performed in Agisoft Metashape software. The steps were implemented as described by Alptekin and Yakar 2020. The results of modelling is shown in Table 2. Digital Surface Map (DSM) (Figure 7) and orthophoto (Figure 8) of the study area were created. Resolution of DSM will be improved with using a UAV that has high resolution.

We import DSM and orthophoto to Virtual surveyor software to draw boundary of pond (Fig 8), point grid and create Triangulated Irregular Network (TIN). We modified TIN until we have satisfied. We import TIN to Netcad software to determine the volume of the pond site. The results are shown in Table 3.

Table 2. Modelling results

Property	Value
Number of images	92
Flying altitude (m)	54.4
Ground resolution (cm/pix)	1.63
Coverage area (km ²)	0.0298
Resolution of camera	4608*3456
Number of GCP	7
Error amount of GCP (cm)	4.92
Resolution DSM (cm/pix)	6.51
Alignment accuracy	Medium
Filtering mode	Aggressive



Figure 8. Boundary of pond

Table 3. Results of the study

Item	Value
3D surface area (m ²)	11404.84
2D surface area (m ²)	9704.39
Volume of pond site (m ³)	31369.34

5. DISCUSSION

Water drought plan has to be prepared as the rainfall regime has been changing. Detailed basin river maps should be prepared for efficiently use the water. To prevent the surface water loss, hydraulic structures should be constructed.

In addition to photogrammetric studies, remote sensing and geotechnical analyses should be carried to design a pond. Permeability and porosity of the soils in the study area should be measured in the laboratory to combine hydrodynamics of the region with the terrain. Groundwater flow pattern has to be determined for using the pond effectively.

In UAV photogrammetry, when the flight height increases, the resolution of each photo decreases. In this study area, there were trees with high elevation near the pond site. UAV may hit to the trees. Therefore, we increased the flight height in flight plan and it caused the decrease in resolution. Manually taken photos with less flight height may give better output.

The coordinates of the GCPs were taken by a GPS. The internet connection in the study area was very weak. Therefore, we took the coordinates with only one epoch. When we have the opportunity to increase epoch number, we will get more precise coordinates. In that case, the error amount of GCP will decrease.

6. CONCLUSION

In this study, volume and 3D surface area of a site that will be used as a pond were calculated using a low-cost UAV. The present study, based on photogrammetric methods, shows that an engineering project can be modelled in a practical way by using a UAV. Geology of the region is very complex. Detailed geological maps should be prepared in order to understand hydrogeological properties of the city. In a master plan, the information of each water retaining structure should be known.

ACKNOWLEDGMENT

We would like to thank to Mersin Provincial Directorate of Agriculture for their help in field studies.

REFERENCES

- Akyıldız M H, Efe H & Önen F (2020). Baraj yapımında atık malzemelerin kullanımı: Kadıköy Göleti Örneği. *DÜMF Mühendislik Dergisi*, 11(1), 439-445. (in Turkish)
- Alptekin A & Yakar M (2020). Heyelan Bölgesinin İHA Kullanarak Modellenmesi. *Türkiye İnsansız Hava Araçları Dergisi*, 2(1), 17-21. (in Turkish)
- Annis A, Nardi F, Petroselli A, Apollonio C, Arcangeletti E, Tauro F, Belli C, Bianconi R & Grimaldi S (2020). UAV-DEMs for Small-Scale Flood Hazard Mapping. *Water*, 12, 1717. DOI: 10.3390/w12061717
- Bilici Ö E & Everest A (2017). 29 Aralık 2016 Mersin selinin meteorolojik analizi ve iklim değişikliği bağlantısı. *Doğu Coğrafya Dergisi*, 22(38), 227-250 (in Turkish).
- Demirkıran O, Köşker Y, Akgül S & Başkan O (2018). Ankara Haymana Kızılköyün Gölet Havzası Sediment Verimi. *Toprak Su Dergisi*, 7(1), 49-56. (in Turkish).
- Dominici D, Alicandro M & Massimi V (2017). UAV photogrammetry in the post-earthquake scenario: case studies in L'Aquila. *Geomatics, Natural Hazards and Risk*, 8(1), 87-103. DOI: 10.1080/19475705.2016.1176605
- Eker R, Aydın A & Hübl J (2018). Unmanned aerial vehicle (UAV)-based monitoring of a landslide: Gallenzerkogel landslide (Ybbs-Lower Austria) case study. *Environmental Monitoring and Assessment*, 190 (28). DOI: 10.1007/s10661-017-6402-8
- Fujihara Y, Tanaka K, Watanabe T, Nagano T & Kojiri T (2008). Assessing the impacts of climate change on the water resources of the Seyhan River Basin in Turkey: Use of dynamically downscaled data for hydrologic simulations. *Journal of Hydrology*, 353, 33-48. DOI:10.1016/j.jhydrol.2008.01.024
- Harmancıoğlu N B, Fedra K & Barbaros F (2008). Analysis for sustainability in management of water scarce basins: the case of the Gediz River Basin in Turkey. *Desalination*, 226, 175-182. DOI:10.1016/j.desal.2007.02.106
- Jia X, Klemeš J J, Alwi S R W & Varbanov P S (2020). Regional water resources assessment using water scarcity pinch analysis. *Resources, Conservation & Recycling*, 104749. DOI: 10.1016/j.resconrec.2020.104749
- Kaya Y, Şenol H İ, Memduhoğlu A, Akça Ş, Ulukavak M & Polat N (2019). Hacim hesaplarında İHA kullanımı: Osmanbey Kampüsü Örneği. *Türkiye Fotogrametri Dergisi*, 1(1), 7-10. (in Turkish)
- Keskiner A D, Çetin M, Şimşek M & Akın S (2020). Kuraklık riski altındaki havzalarda gölet haznelerinin tasarımı: Seyhan Havzası'nda bir uygulama. *Teknik Dergi*, 586, 10189-10210. DOI: 10.18400/tekderg.505584
- MÇŞİM (Mersin Çevre ve Şehircilik İl Müdürlüğü) (2018). Mersin ili 2017 yılı çevre durum raporu. (in Turkish)
- MTA (2009). Geological Map of the Mersin-033 Quadrangle. Ankara, Turkey
- Orhan O & Yakar M (2016). Investigating Land Surface Temperature Changes Using Landsat Data in Konya, Turkey. *The International Archives of the Photogrammetry, Remote Sensing and Spatial Information Sciences*, XLI-B8, 285-289. DOI: 10.5194/isprsarchives-XLI-B8-285-2016
- Orhan O, Yalvaç S & Ekercin S (2017). Investigation of Climate Change Impact on Salt Lake by Statistical Methods. *International Journal of Environment and Geoinformatics*, 4(1) 54-62.
- Orhan O, Dadaser-Çelik F & Ekercin S (2019). Investigating land surface temperature changes using Landsat-5 data and real-time infrared thermometer measurements at Konya closed basin in Turkey. *International Journal of Engineering and Geosciences*, 4(1), 2019. DOI: 10.26833/ijeg.417151
- Özgül N (1983). Stratigraphy and tectonic evolution of the Central Taurides. *International Symposium on the Geology of the Taurus Belt*, Ankara, Turkey, 77-90
- Sarro R, Riquelme A, García-Davalillo J C, Mateos R M, Tomás R, Pastor J L, Cano M & Herrera G (2018). Rockfall Simulation Based on UAV Photogrammetry Data Obtained during an Emergency Declaration: Application at a Cultural Heritage Site. *Remote Sensing*, 10, 1923. DOI: 10.3390/rs10121923
- Şasi A & Yakar M (2018). Photogrammetric modelling of hasbey dar'ülhuffaz (masjid) using an unmanned aerial vehicle. *International Journal of Engineering*

- and Geosciences, 3(1), 6-11. DOI: 10.26833/ijeg.328919
- Swain S S, Mishra A, Sahoo B & Chatterjee C (2020). Water scarcity-risk assessment in data-scarce river basins under decadal climate change using a hydrological modelling approach. *Journal of Hydrology*, 125260. <https://doi.org/10.1016/j.jhydrol.2020.125260>
- Ulvi A (2018). Analysis of the utility of the unmanned aerial vehicle (uav) in volume calculation by using photogrammetric techniques. *International Journal of Engineering and Geosciences*, 3(2), 43-49. DOI: 10.26833/ijeg.377080

- Ulvi A & Yiğit A Y (2019). Kültürel Mirasın Dijital Dokümantasyonu: Taşkent Sultan Çeşmesinin Fotogrametrik Teknikler Kullanarak 3B Modelinin Yapılması. *Türkiye Fotogrametri Dergisi*, 1(1), 1-6. (in Turkish)
- Ulvi A, Yakar M, Yiğit A Y & Kaya Y (2020). İHA ve Yersel Fotogrametrik Teknikler Kullanarak Aksaray Kızıl Kilise'nin 3 Boyutlu Nokta Bulutu ve Modelinin Üretilmesi. *Geomatik Dergisi*, 5(1), 19-26. DOI:10.29128/geomatik.560179 (in Turkish)



© Author(s) 2020. This work is distributed under <https://creativecommons.org/licenses/by-sa/4.0/>



Investigation of The Rainwater Harvesting Potential at the Mersin University, Turkey

A. Yasin YİĞİT¹, Osman ORHAN^{*2}, Ali ULVİ²

¹Mersin University, Faculty of Engineering, Department of Geomatics Engineering, Mersin, Turkey

²Mersin University, Department of Remote Sensing & GIS, Mersin, Turkey

Keywords

Rainwater harvesting
UAV
Irrigation
Classification

ABSTRACT

The rapid population growth in the world and the adverse effects of climate change, has caused a severe increase in water demand used in sectors such as agriculture, industry, and domestic usage. The fact that the water resources in the world are stable and their availability is limited, the importance of water resources, efficient use of water, and the use of technologies related to alternative water resources have become important. This study aimed to investigate the usage potential of rainwater to be collected from the roofs of the building in irrigation of green areas in Mersin University - Çiftlikköy campus. For this purpose, first, whether the roofs inside the campus can collect rainwater will be revealed with unmanned aerial vehicles. Then, appropriate roof areas where rainwater will be collected will be calculated using the object-based classification method. The rainwater amounts to be collected from each building will be calculated using the monthly precipitation data obtained from the Provincial Directorate of State Meteorology Affairs. In addition, by calculating the number of green areas on the campus and the need for rainwater, it was determined how much rainwater to be collected meets the water need according to different irrigation periods.

1. INTRODUCTION

In general, greenhouse gases increase, and greenhouse gas effects are strengthened due to various human activities such as burning fossil fuels, land-use change, deforestation, such as. The increase in greenhouse gases in the atmosphere causes global warming and as a result, climate change occurs (Trenberth, 2011; Olaniyi et al., 2019). Recently, excessive, and unconscious use of resources has caused global warming, which has brought climate changes. Due to climate change, temperature increases and changes in precipitation regimes have come to the fore. Climate change: affects stream flows, groundwater, and water volumes in lakes depending on changes in temperatures and precipitation. This effect does not have a regular process; It causes a decrease in precipitation in winter, sudden precipitation in summer, and above or below seasonal temperature averages (Sandalcı, 2011).

Water, which is the main element of life, is a very effective substance not only in the living environment but also in the inanimate environment. Natural

phenomena such as the formation of soil by physically breaking the rocks, the fertility of the soil by dissolving the substances in it, the emergence of plants, the transportation of the necessary building blocks from the roots to the leaves on the branches, and photosynthesis take place through the water. "Life started in water". The proposition is indicative of the importance of water on earth. Although 97.5% of the world is covered with water, only 2.5% of this water is usable. Considering that 2% of this limited amount is found at the poles as ice masses of 16 km thickness, only 0.5% of the water is usable (Ulusoy, 2007).

When countries are classified according to water availability, countries with an average amount of usable water less than 1000 m³ per year are water-poor countries, countries with 1,000-3,000 m³ water shortages, countries with 3,000-10,000 m³ water, less than 10,000 m³. And the countries with high levels are considered water-rich countries (Alparslan et al., 2008; Şahin and Manioğlu 2011). The amount of water available per person per the year 1500-1600 cubic meters. Turkey is a country suffering from water shortages. Because Turkey's population is expected to

* Corresponding Author

(ayasinyigit@mersin.edu.tr) ORCID ID 0000-0002-9407-8022
*(osmanorhan44@gmail.com.tr) ORCID ID 0000-0002-1362-8206
(aliulvi@mersin.edu.tr) ORCID ID 0000-0003-3005-8011

Cite this article

Yiğit A Y, Orhan O & Ulvi A (2020). Investigation of The Rainwater Harvesting Potential at the Mersin University, Turkey. Mersin Photogrammetry Journal, 2 (2), 64-75

rise to 87 million over the next 20 years. With the increase in the population, it is estimated that the amount of water per person will decrease to 1042 cubic meters. In this case, in terms of the future, Turkey will be a candidate to be one of the most water-poor countries (Eren et al., 2016; SFR, 2017).

Studies have been conducted to examine the impact of climate change on hydrology by focusing on the water cycle and water resources on human and environmental water use. One of these studies is rainwater harvesting. Only 30% of rainwater is added to groundwater, and the remaining 70% cannot be utilized (Kılıç, 2008; Haddeland, 2014). Rainwater harvesting is the collection and accumulation of rainwater and runoff water, and water provision required for domestic consumption through vegetable-animal production (Oweis et al., 2001; Kantaroğlu 2009). Rainwater collected by pipes from open areas such as roads, sidewalks, and parking lots, especially on residential roofs, is filtered and then stored in the tank and this water is stored in garden irrigation, car washing, toilet reservoir, cleaning works, etc. can be used for needs (Eren et al., 2016; SFR, 2017). As a result of the collection, storage, and use of rainwater in this way, both water resources are protected, and economic gain is obtained.

The use of rainwater to meet alternative water needs is of great importance in water-saving and the protection and sustainability of water resources. When we look at the rain harvesting studies in the world, many concrete cisterns have been built in Thailand since the eighties, and the water collected here is used for drinking and use (Kılıç and Babuş, 2018). In the United States of America, approximately 250,000 houses have rainwater harvesting systems (Alparslan et al., 2008). In some islands in the Caribbean, a rainwater collection system is included in new structures (İncebel 2012). The use of gray water treatment systems or rainwater collection systems in buildings larger than 30,000 m² in Japan has been made mandatory by the Japanese Ministry of Public Works (Kılıç and Babuş, 2018). According to DIN (1989), in Germany, standards for rainwater collection systems, planning, installation, implementation and maintenance, rainwater filtration, rainwater reservoirs, and additional components are discussed (Sturm et al., 2009). New York World Trade Center. In this skyscraper, rainwater is collected on the roof and stored for irrigation of the surrounding park and cooling of this building, which saving 25% in energy used in building cooling (Tıkansak, 2013; Tanık, 2017). Frankfurt Airport Terminal B is used for rainwater, irrigation, and toilet washing. Germany Marburg Tennis Court is irrigated with rainwater supplied from outside (Tanık, 2017). In the United States, it is known that there are rainwater storage systems in 100,000 homes. It is known that most of these are for garden irrigation and plant growth, and 20% of them are for drinking water. (Dorak, 2015; Tanık, 2017). There are various examples of rainwater harvesting technology from building roofs in our country. Many technologies related to water conservation have been developed in the "Green Building Concept" in the Siemens Gebze Organized Industrial Zone. Rainwater collected from the roof can

be used in the fire irrigation system, softened and used as utility water in the whole area, and used in landscape irrigation outside the building. The rainwater collected from the roofs and coming to the water tank in Diyarbakır Solar House and the water obtained from domestic wastewater treatment are used in garden irrigation and toilet reservoirs by passing through a carbon filter. Rainwater collected from roofs at Borusan Oto İstinye Facilities is collected and treated in separate tanks and used in toilet reservoirs, vehicle washing, garden irrigation, and fire depot (Şahin and Manioğlu, 2011). Overall Turkey's examples regarding the use of rainwater, which is water-saving strategies to reduce water consumption in buildings, are seen as quite limited.

This study, it was aimed to investigate the potential of rainwater that can be collected from building roofs for irrigation of green areas in Mersin University Çiftlikköy campus and to determine its usability for greenfield irrigation needs. In this context, building roofs were detected by using multi-spectral UAV images to detect roof areas of the building. The object-based classification method has been used in the determination of building roofs.

With the development of technology, data collection methods have also improved, and especially image-based data have started to provide more detailed information in it (Demirel, 2010; Kavzaoğlu and Çölkesen, 2010; Demir, 2012; Kaya, 2020; Arasan et al., 2020; Saritur et al., 2020). The density of the data obtained made it necessary to infer the meaningful ones in these data. Previously, the extraction of the desired details was done manually by the operators. This extraction and classification process, which has been done manually for many years, has become faster and easier thanks to the developing detail extraction methods.

If pixel-based approaches are applied to obtain information from remotely sensed data, only spectral information is used. Therefore, pixel-based approaches cannot meet high-resolution image classification and information extraction is based solely on gray level thresholding methods, requiring the user to deal with big data. In this case, the pixel-based classification method applied in high-resolution images with rich information content, buildings, roads, parks, etc. Precise data extraction from urban areas with strict boundaries makes it very difficult. This deficiency has brought along advanced image analysis and classification approaches depending on the existing computing technologies. Therefore, in today's image processing and remote sensing technologies, object-based classification approaches have been used extensively (Baatz et al., 2004; Bacher and Mayer, 2005; Marangoz, 2009; Bilgilioğlu, 2015; Yiğit and Uysal, 2019a; Yiğit and Kaya, 2020).

An object according to the object-based classification approach; is defined as a group of pixels with similar spectral and spatial properties. In this approach, segments representing objects; shape, texture, neighborhood relationship, morphological relations, area, height value, distance, geometric shape, standard deviation, density, and so on. It is analyzed

using values and assigned to target classes. Most of this information is specific to the object-based classification method, they cannot be used in the pixel-based classification method. More accurate classification results are obtained by using different properties of the object (Hofmann and Jain, 1987).

Kabadayı and Uysal (2020) detected buildings using high-resolution UAV images. They first subjected the digital products they produced from the UAV data to the segmentation process and then classified them using various indexes. Karlı et al. (2010), aimed to automatically extract building details from infrared aerial photographs. They pointed out that when it comes to object detection, segmentation is of great importance in image processing and computer vision techniques. Therefore, three different segmentation methods were used to extract building and road details. In their work, they revealed that building details can be determined automatically from infrared aerial photographs. Grigillo and Kanjir (2012) aimed to automatically extract buildings in cities and cities in an object-based manner in their study. They produced Normalized Digital Surface Model (nSYM) by producing Digital Surface Model (DSM) and Digital Terrain Model (DTM) produced from Lidar and digital images. The object-based classification method was chosen, and they preferred the multi-resolution segmentation method.

Kalkan and Maktav (2010) compared the object and pixel-based classification methods they made on satellite images. Since pixel-based classification is based only on the statistical analysis of pixels, they grouped the pixels in the segmentation stage and mentioned that these segments give more meaningful and positive results for the thematic class in the object-based classification method, which uses many properties such as color, frequency, and neighborhood. As a result of the study, they compared object and pixel-based classification methods. They stated that both pixel and object-based gave success results, and they obtained better results in high-resolution images thanks to the segmentation process used in the object-oriented classification method.

Firat and Erdoğan (2015) carried out an automatic detail extraction study by using multispectral aerial photographs and DSM and DTM in the object-based classification method. In the scope of the study, automatic extraction of vegetation cover and water surface details, especially the building, was examined. They used the height model and the Normalized difference vegetation index (NDVI) index for object extraction. It has been observed that the values entered by the operator just before the segmentation stage, which is the most important stage in object-based classification, affect the accuracy. For example; It was stated that the extraction of buildings was a success of

81%, and the buildings that could not be detected were small buildings and the reason for this was the scale parameter. As a result, it was stated that automatic object extraction from aerial photographs with object-based classification method was successful but using images with multispectral bands alongside SAM and DEM data would increase accuracy.

Since high-resolution UAV images are used in this study, the object-based classification method was preferred. In addition, since a large part of the study area consists of low green areas and forest areas, UAV images with Near-infrared (NIR) band have also been used, which contributes to higher accuracy in determining green areas.

Green areas, buildings, and roads were determined by the object-based classification method from digital products (Orthophoto-DSM-DTM) produced from images with Red-Green-Blue-NIR-Rededge (R-G-B-NIR-Redge) bands taken by UAV. Thanks to automatic detail detection, data clutter has been eliminated and the analysis process in large areas has become easier. After the determined buildings, the building roof areas were calculated. Then, the total amount of rainwater was calculated, and it was also investigated that what percentage of the irrigated green areas would be covered by rainwater if irrigated every day, once a week, and twice a week.

2. STUDY AREA

Mersin University located in Mersin city has nine campuses. Çiftlikköy Central Campus, the main campus site, was built in 1992. Çiftlikköy Campus, 14 kilometers away from the city center, has an area of 4 181 097 m². (Fig. 1).

A great deal of campus area is vegetated land and natural environment. University Administration takes measures in preserving natural habitat and forests. Mersin University gives priority to increasing the total forest area (1 363 873 m²) and planted vegetation area. In the current state, the area of vegetation that needs to be irrigated is 319552 m² while the built-up area (roof area of buildings) in total is 125 427 m² derived from UAV data. The rest of the campus area is designed and used for sports fields, pavements, and parking. Mersin University master plan aims to preserve natural habitat and water-absorbing land as one of the pillars of green campus planning. In this manner, limited development is planned for buildings and built-up areas.

Çiftlikköy Campus is among the privileged campuses with its original architectural design (Demirci & Özdemir, 2020) and contemporary arrangements, large and eye-catching buildings, green and forest areas, many social, cultural and sports facilities. It is one of the attractive campus sites in Turkey.



Figure 1. The Study area (White polygon shows the boundry of Mersin University)

3. MATERIEL and METHOD

Digital products were produced using images taken with a UAV belonging to the campus area. With these, buildings were automatically detected with the object-oriented classification approach. The UAVs used in the study for this purpose and technical information are given in Figure 2, Table 1 and 2, respectively.

A total of 1808 photographs were collected with the Parrot Bluegrass UAV from a height of 80 meters from a rare location and double grid (Figure 3). With the Sensefly + UAV, a total of 842 photographs were collected from a height of 120 meters from a rare location and overlapped (double grid).



Figure 2. UAV (A: Sensefly Ebee Plus UAV and S.O.D.A Camera B: Parrot Bluegrass UAV and Parrot Sequoia+ Camera)

Table 1. Parrot Bluegrass UAV and Parrot Sequoia + Camera basic technical features (Paksoy teknik, 2020a)

Specialty	Value
weight	1810 g
cruising speed	2-20 m/s
Max of flight time	About 25 minutes
Radiolink distance	2 km
Satellite Positioning Systems	+
Camera model	Parrot Sequoia+
Sensor type	R-G-Redge-NIR (14 mp)
4 x sensors Focal length	3.98 mm
RGB Focal length	4.88 mm

Table 2. Sensefly Ebee Plus UAV ve S.O.D.A Camera basic technical features (Paksoy teknik, 2020b)

Specialty	Value
Weight/ Size	1100 g /1100 mm
Cruising speed	40-110 m/s
Max of flight time	About 50 minutes
PPK/RTK	+
Radiolink distance	3 km
Satellite Positioning Systems	+
Sensor type/ Sensor size	R-G-B (20 mp)/ 1-inch
Resolution/ Focal Length	5472x3648/10.6 mm

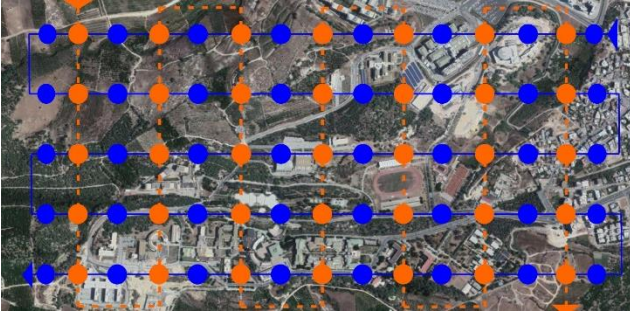


Figure 3. Double Grid Flightpath (Line: Flight Path – Circle: Sample photos) (UAV flight software: Emotion software for Ebee Sensefly, Pix4D Capture software for Parrot Bluegrass).

Besides, ground control points (GCP) were measured with a Global Navigation Satellite Systems (GNSS) device to bring the photogrammetric products obtained within the scope of the study to the same location as the ground location (Şasi & Yakar, 2018; Ulvi et al., 2020). Using these surveyed GCPs, digital maps have been brought to their real position (Spatial referencing has been made). For this process, a total of 32 YKNs, 20 of which are ground-centered in the campus and 12 on buildings and similar high-rise buildings, have been founded and measured.

3.1. Photogrammetric Process

Photogrammetry is a technique used to create digital maps that allow obtaining reliable measurements and information of physical objects by recording, measuring, and interpreting photographs or images obtained with metric cameras or unique sensor systems (Kraus, 2011).

One of the methods adopted in recent years to collect the spatial data needed is UAVs. With UAV technology, data of large areas can be collected faster and at a low cost. To produce a digital map of Mersin University Çiftlikköy Campus, flights were made with an MS sensor (Red-Green-Rededge-NIR) UAV and RGB (red-GreenBlue) sensor UAV. First of all, GCPs have been placed on the land to ensure that the obtained products coincide with the actual land location.

The images collected with the UAV are orientated with photogrammetric valuation software (Pix4d Mapper). At the end of the orientate, it was converted into a national coordinate system using GCPs measured from the field. Later, the orthophoto of the study area, DSM and DTM were produced.

In the study, since the rainwater to be collected on the roof building's roofs will be calculated and to obtain more precise location and height information, homogeneous distribution in the GCP facility was emphasized. A total of 32 GCPs were installed within the campus boundaries, 20 of which were installed at the ground center and 12 on the building's roofs. According to the terrain model, double grid flight planning was done by flying the MS sensor UAV from 80 meters. A total of 12 flights were carried out in the study area, and 1808 photographs were taken. Also, flights were made with an RGB sensor UAV from 120 meters, and 842 photographs were taken in 6 flights in total.

3.2. Object-Based Images Analysis

Object-oriented image analysis method; the shape, color, texture, etc. in the image analyze specific properties. It provides a system that captures objects according to their distinctive features (Bilgiliöglu, 2015). This method: provides the ability to distinguish various objects in the image such as buildings, trees, roads, and vehicles. The object-based classification method includes segmentation and classification stages (Bergsjö, 2014). While the segmentation process allows the target classes on the image to be collected in the same segment, the second stage requires the classification of objects (Yiğit and Uysal, 2019a).

The most important and first step in object-based classification is segmentation.

Segmentation is the process of grouping pixels with similar spectral properties and creating image objects. The purpose of segmentation is to divide the image into different subsections and create meaningful objects (Baatz et al., 1999; Yiğit and Uysal, 2019b).

There are various segmentation methods in the literature. In this study's multi-resolution segmentation algorithm, image objects are divided into small pieces based on average heterogeneity for a given resolution. The heterogeneity criterion must be below a certain threshold. Weight parameters determine color and shape heterogeneity.

Color shape and compactness parameters are necessary for good image segmentation. Also, the scale parameter is required to stop the optimization process. The difference in heterogeneity is calculated before joining two adjacent objects. When the increment exceeds the threshold set by the scale parameter, the object join process is stopped and the partitioning is completed.

In the multi-resolution segmentation algorithm, the parameters are set by the user. These parameters are scale, color/shape, and softness/density. The parameters should be entered as close to the truth as possible. The most important of the 3 parameters entered is the scale parameter. The softness/density and Color/shape parameters complement each other to 1.

The Color and Shape criteria generate image objects consisting of relatively homogeneous pixels using the general Segmentation Function (SF) formulated in equation (1).

$$Sf = w_{color} h_{color} (1 - w_{color}) h_{shape} \quad (1)$$

where the user-defined weight for spectral color or shape is $0 < w_{color} < 1$.

Spectral (i.e., color) heterogeneity (h) of an image object is computed as the sum of the standard deviations of spectral values of each layer (σ_k) (i.e., band) multiplied by the weights for each layer (w_k):

$$h = \sum_{k=1}^m w_k \cdot \sigma_k \quad (2)$$

The color criterion is computed as the weighted mean of all changes in standard deviation for each band k of the m bands of remote sensing dataset. The standard deviation is σ_k weighted by the object sizes n_{ob} (i.e. the number of pixels):

$$h_{color} = \sum_{k=1}^m w_k [n_{mg} \cdot \sigma_k^{mg} - (n_{ab1} \cdot \sigma_k^{ab1} + n_{ab2} \cdot \sigma_k^{ab2})] \quad (3)$$

(where mg means merge).

Compactness:

$$c_{pt} = \frac{l}{\sqrt{n}} \quad (4)$$

Smoothness:

$$smooth = \frac{l}{b} \quad (5)$$

(Karakış et al., 2006)

n is number of pixels in the object, l is the perimeter, b is shortest possible border length of a box bounding the object

$$h_{cpt} = n_{mg} \cdot \frac{l_{mg}}{\sqrt{n_{mg}}} - \left(n_{ob1} \cdot \frac{l_{ab1}}{\sqrt{n_{ab1}}} + n_{ab2} \cdot \frac{l_{ab2}}{\sqrt{n_{ab2}}} \right) \quad (6)$$

$$h_{smoth} = n_{mg} \cdot \frac{l_{mg}}{b_{mg}} - \left(n_{ob1} \cdot \frac{l_{ab1}}{\sqrt{n_{ab1}}} + n_{ab2} \cdot \frac{l_{ab2}}{\sqrt{n_{ab2}}} \right) \quad (7)$$

$$h_{shape} = w_{cpt} \cdot h_{cpt} + (1 - w_{cpt}) \cdot h_{smoth} \quad (8)$$

After the images were separated into meaningful segments, each segment's properties were tested, and the responses of each feature in each image band and image segment were analyzed. The analysis led to the determination of the boundary values that would best represent the class based on the feature that captured the associated class distinction.

Thus, the classification continued with the limits set in the relevant membership function, and this stage was made cyclically until the best classification representing real-world conditions was obtained.

The software has two basic classifications. These are fuzzy membership and nearest neighborhood functions. In the nearest neighbor classification function, the user defines classes using sample objects for each class. In the fuzzy membership classification function, the ranges of the properties of objects belonging to a specific class or where they do not belong are defined.

In the classification phase, values belonging to the building-green area-road class were determined first. Then, classes were created by determining the properties of objects that do not belong to these classes. It was seen that some segments were assigned to the wrong class after the assignments to the classes were delayed. Merge and border reshaping operations were applied after the segments assigned to the wrong classes were assigned to the correct class. The indices used in the classification process are shown in Table 3. In the study, four class assignments were made with object-based classification as buildings, green areas, roads, and others.

Finally, an accuracy analysis was conducted to determine the compatibility of the classes with the real space. Accuracy analysis is the last step in measuring the accuracy and reliability of the classification. In order to check the classification quality and accuracy, the most common accuracy estimation parameters, general accuracy, manufacturer accuracy, user accuracy, and Kappa coefficient, were calculated using the TTA mask-based error matrix approach (Lu et al., 2004). TTA is a file called training and testing area mask that contains information about the classes created, allowing them to transfer existing samples to other scenes (Yiğit and Uysal, 2020). Building data obtained by geodetic methods were used as reference data sources (Base map made using GNSS and Total Station).

Table 3. RGB- Rededge-NIR band indices used in this study

Name	Index Name	Formula	Reference
GRVI	Green-red vegetation index (The Synthetic NDVI)	$\frac{(Green - Red)}{(Green + Red)}$	Motohka et al., 2010
RRI	Red ratio index	$\frac{(Red)}{(Blue + Green + Red)}$	Çömert et al., 2017
GRI	Green ratio index	$\frac{(Green)}{(Blue + Green + Red)}$	Sonntag et al., 2012
CBR	Common Band Ratio	$\frac{Blue + Green + Red}{3}$	Çömert et al., 2017
NDVI	Normalized Difference Vegetation Index	$\frac{NIR - Red}{NIR + Red}$	Rouse Jr et al., 1974
DDVI	Difference Difference Vegetation Index	$[(2 \times NIR - Red) - (Green - Blue)]$	Eisfelder, 2009
TDVI	Transformed Difference Vegetation Index	$1.5x \frac{NIR - Red}{\sqrt{NIR^2 + R + 0.5}}$	Bannari et al., 2002
$NDVI_{Rec}$	Red-edge NDVI	$\frac{NIR - Rededge}{NIR + Rededge}$	Gitelson and Merzlyak, 1994

3.3. Rainwater Efficiency Calculation

The Calculations for how much rainwater will be collected from the roof surface are summarized below (Eren et al., 2016; Kılıç and Abuş, 2018; Tema 2020).

Roof area: a functional area (m²) where rainwater can be collected.

Precipitation amount: It is the total annual precipitation amount determined by the General Directorate of Meteorology.

Roof coefficient (Yield Coefficient): German standards specify the coefficient as 0.8 in DIN (1989). The roof coefficient means that all the rain falling on the roof cannot be recycled. Filter efficiency coefficient: The coefficient specified by German standards as 0.9 in DIN (1989). The filter efficiency coefficient is the efficiency coefficient of the first filter passed to separate rainwater obtained from the roof from visible solids. It is a coefficient given by calculating that some water cannot pass through here. As a result, it is calculated by the formula below.

$$Rainwater_{harvesting} (m^3) = \frac{roof}{area} \times \frac{roof}{coefficient} \times \frac{filter}{efficiency} \times coefficient \times \frac{Precipitation}{amount} \left(\frac{mm}{year}\right) \quad (9)$$

$$Rainwater_{harvesting} (m^3) = \frac{roof}{area} (m^2) \times 0.9 \times 0.8 \times \frac{Precipitation}{amount} \left(\frac{mm}{year}\right) \quad (10)$$

4. RESULT and DISCUSSION

4.1. Photogrammetric Process

As a result of the images obtained with the Multispectral UAV and RGB UAV, ortho-mosaics belonging to the R, G, B, Red edge, NIR bands of the study area were produced. Besides, DTM and DSMs belonging to the region were obtained. The Ground Sample Distance (GSD) of orthophotos produced has a resolution of 2.7 cm. What is the mean, the real terrain equivalent of the distance between the centers of adjacent pixels in digital images is called GSD. The orthophoto and digital surface model (DSM) of the study area are shown in Figure 4.

In addition, Digital Terrain Model (DTM) was produced with Virtual Surveyor software. In this software, an orthophoto of the area and any DSM map are required to produce DTM. With these maps, points for the DTM map are generated automatically or manually. Then, a DTM map is obtained with these points.

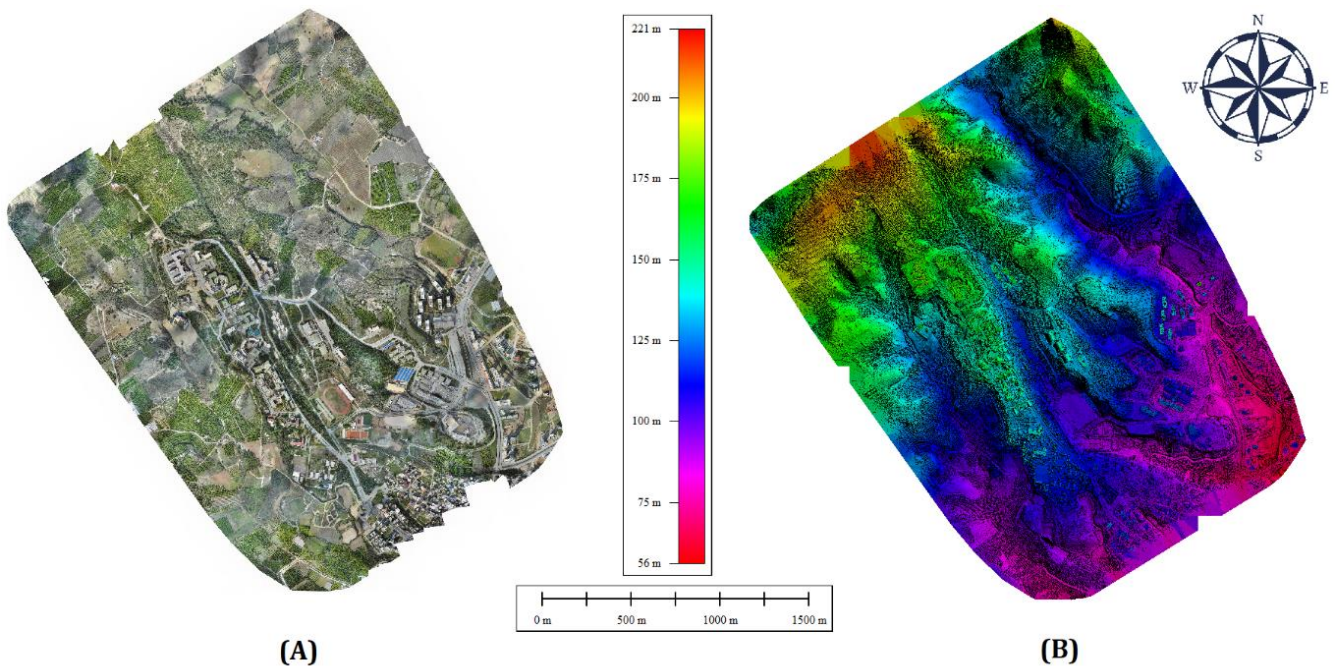


Figure 4. Digital map of the study area (A) Orthophoto (B) DSM

4.2. Detection of building roof areas

After producing digital maps (Orthophoto-DSM-DTM), the nDSM (Normalized digital surface model), the most preferred input product in building extraction, was first created. DSM-DTM formula is applied for the nDSM model.

After the digital maps were produced (Orthophoto-DSM-DTM-nDSM), the detailing extraction was started in the Definiens eCognition software. First, the segmentation process was applied to create meaningful objects from digital images. Before starting the

segmentation process, scale, softness/density, and color/shape parameters were determined. These three parameters entered in the segmentation stage were tried under different criteria, and 120 were selected for scale parameter, 0.6 for compactness parameter, and 0.4 for shape parameters. The segmentation result, according to the selected parameters, is shown in Figure 5.

After the segmentation process, the detail extraction and classification process was initiated. See Table 3 to look at the indices used in the classification process, and the classes created are shown in Figure 6.

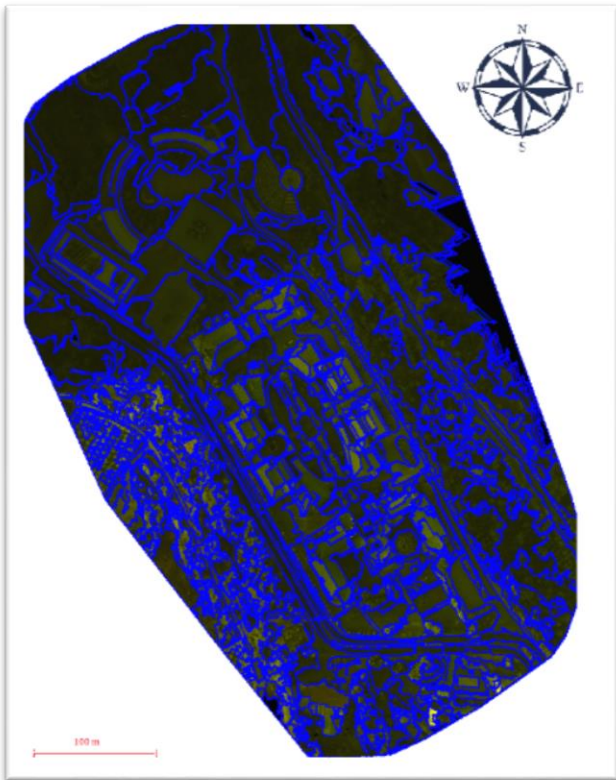


Figure 5. Segmentation result product (Sample area: Engineering faculty)

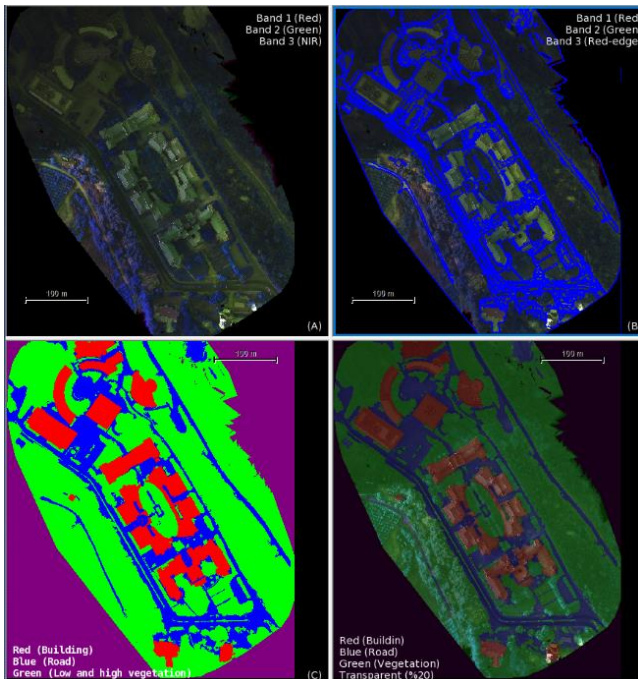


Figure 6. Classification steps for engineering faculty which is one of the sample areas. A: Input data, B: merged segmentation, C, and D: Classification results.

After the classification process, to check the classification quality and accuracy (for building roofs), the accuracy estimation parameters, general accuracy, manufacturer accuracy, user accuracy, sensitivity, originality, and Kappa coefficient were calculated (Table 4). Building data obtained by geodetic methods were used as reference data sources.

Table 4. Accuracy assessment by the TTA mask and random points analysis

General Accuracy	Producer Accuracy	Users Accuracy	Precision	Specificity	Kapa
0.919	0.872	0.859	0.916	0.893	0.904

With the object-based classification method, buildings are automatically detected quickly and with high accuracy. Finally, building roof boundaries have been simplified with the "Simplify Building" command in the GIS (Geographic information system) software (Arcgis) to generalize product data. Buildings where rain harvesting is possible and areas that need irrigation are shown in figure 7.

Eren et al. (2016) aimed to investigate the use potential of rainwater collected from building roofs in their university studies. Using the map drawing program, the total roof areas of the buildings and the size of the green areas in each zone were calculated. However, within the scope of the study, no details were given about the provision of digital data on building roofs. Roofs of buildings may have been obtained from existing projects, digital plan data, or digitization from platforms such as Google Earth.

Utsav et al. (2014) constitutes another example of a university. The study was carried out at Sankalchand Patel University Visnagar campus. In the study, it was mentioned that the total basin area was calculated and data for all the buildings of the campus were collected. But the method is not specified. In this study too, there is no information about how data on buildings and roofs are obtained.

Building roofs were detected using high-resolution UAV (in the study) or satellite imagery (Hacar, 2020; Orhan & Yakar, 2016) data without the need for any plan or digital data. In our study, unlike the literature, the data of the buildings were obtained from high-resolution images without using any plan data. In this way, the potential for rain harvesting of large zone or areas can be easily determined and a new perspective has been given to rain harvesting studies on building roofs.

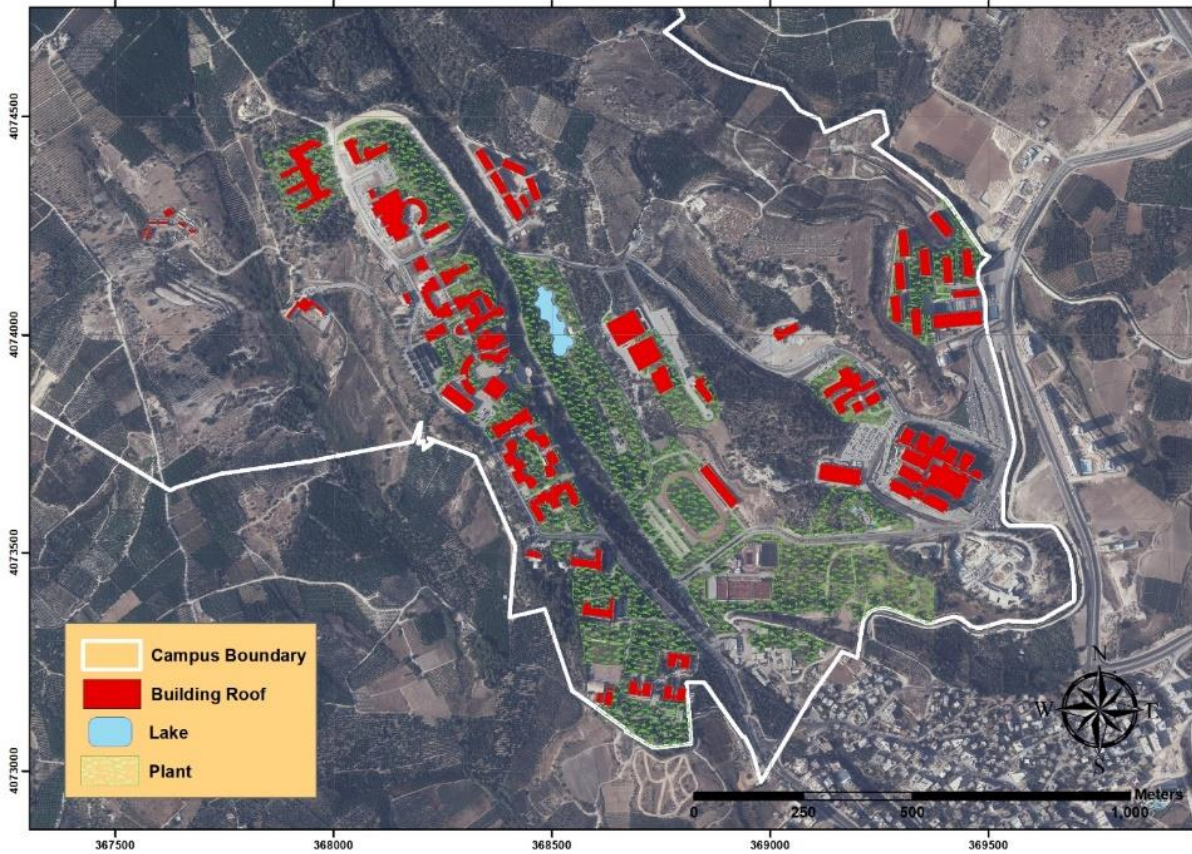


Figure 7. Roof areas suitable for rain harvesting and irrigated green areas.

4.3. Rainwater harvest

The last 30 years' data of the meteorology station located in the study area was obtained from the Turkish State Meteorological Service, and accordingly, it was seen that the annual rainfall was 655 mm (655 l/m²). In addition, as a result of the object-based classification process, the roof area of the buildings within the campus boundaries was determined as 125 427 m².

Rainwater harvesting:

$$125\,427\,m^2 \times 655\,l/m^2 \times 0.8 \times 0.9 = 59\,151\,373\,L$$

$$= 59\,151\,m^3/year$$

4.4. Calculation of the amount of water required for green field irrigation;

Considering the diversity of vegetation in the campus, it was found that although there are trees, there are generally leafy shrub and grass. In addition, considering the irrigation areas, it was determined that most of them were leafy shrub and grass. The irrigation need of leafy shrub is 8.25 mm / day (8.25lt / m²), and the irrigation need of grass is 7.25 mm / day (7.25lt / m²) in hot climatic regions (Erdoğan, 2002). Since it is known that the shrub and grass are of equal density, this

value is taken as 7.75 mm / day (7.75 l / m²) for the working area.

The green areas within the campus boundaries were extracted as a result of the Object-based classification process. However, during the field study, it was noticed that not all these areas were irrigated or that certain areas (forest) did not need irrigation. For this reason, only the green vegetation (leafy shrub and grass) areas where irrigation is carried out were corrected with the help of local measurements. As a result of the correction, the irrigation areas within the campus boundaries were determined as 319 552 m².

The daily amount of water for irrigation:

$$319\,552\,m^2 \times 7.75\,l/m^2 = 2476528\,l = 2477\,m^3/day$$

Irrigation water needs are calculated separately for cases where irrigation is done every day, twice a week and once a week, and are given in Table 5. It has been determined that the amount of water collected from the roof areas will meet 6.5% of the total garden irrigation water if irrigation is done every day, 23% of the total garden irrigation water if irrigation is done twice a week, 45.8% of the total garden irrigation water if irrigation is done once a week.

Table 5. Irrigation needs and efficiency values according to different irrigation periods

Amount of rainwater collected (m ³ /year)	The daily amount of water for irrigation (m ³)	once every day		twice every week		once every week	
		Total water requirement (m ³)	Percentage of water met (%)	Total water requirement (m ³)	Percentage of water met (%)	Total water requirement (m ³)	Percentage of water met (%)
59 151	2 477	904 105	6.5	258316	23	129 158	45.8

5. CONCLUSION

In this study, rainwater as an alternative water resource was emphasized and information about rainwater harvesting was given. In addition, the roof areas were automatically extracted using the object-based classification method with the help of UAV data. This situation sets an example for extracting building areas at the regional, district or local scale and easily determining the region's total rainwater harvesting potential.

In the Mersin University rainwater harvesting study, 59 151 m³ / year usable rainwater is obtained from the roofs of the existing 125 427 m² buildings. It has been demonstrated that the collected rainwater can be saved up to 46% if the water need of 319 552 m² of green area, which is irrigated regularly in the campus, is met once every week.

70% of the water consumed for drinking and utility purposes is used for toilets, garden irrigation, car-washing and laundry. Only 30% of the rainwater goes into groundwater, and the remaining 70% goes directly into the sewage. Considering the importance of water for living things, it becomes clear how important it is to evaluate rainwater (Eren et al., 2016; Kılıç and Abuş, 2018). Considering the results obtained from the study, it is seen that storing rainwater and using it in green area irrigation is of great importance in terms of sustainable use of existing water resources and saving water. By extending these systems, ecological balance will be preserved, sustainable development will be ensured, and water resources will be used more efficiently. For this reason, the importance of collecting and using rainwater in buildings should be explained to all members of society, and every individual should be encouraged in this regard.

ACKNOWLEDMENT

This study was supported by Mersin University Scientific Research Projects Coordination Unit (Project Number:2020-1-AP5-3836).

REFERENCES

Alparslan N, Tanık A & Dölgen D (2008). Türkiye’de Su Yönetimi Sorunlar ve Öneriler. Türk Sanayicileri ve İşadamları Derneği (TÜSİAD) Yayın No: T/2008-09/469. Ankara

Arasan G, Yılmaz A, Fırat O, Avşar E, Güner H, Ayğın K, Yüce D (2020). Accuracy Assessments of Göktürk-1 Satellite Imagery. *IJEG*, 5 (3), 160-168.

Baatz M & A Schäpe (1999). Object-oriented and multiscale image analysis in semantic networks. In: Proc. Of the 2nd International Symposium on Operationalization of Remote Sensing, August 16th-20th, Enschede. ITC.

Baatz M, Benz U, Dehghani S, Heynen M, Höltje A & Hofmann R (2004). eCognition Professional: User Guide 5, Definiens-Imaging, Munich.

Bacher U & Mayer H (2005). Automatic road extraction from multispectral high resolution satellite images. *IAPRS*, 36, Vienna, Austria, August 29-30, 2005.

Bannari A, Asalhi H & Teillet P M (2002). Transformed difference vegetation index (TDVI) for vegetation cover mapping. In *IEEE International geoscience and remote sensing symposium* (Vol. 5, pp. 3053-3055). IEEE.

Bergsjö J (2014). Object based change detection in urban area using KTH-SEG. Bachelor Thesis, Kth Royal Institute Of Technology, Stockholm.

Bilgilioğlu B B (2015). Uzaktan algılanmış görüntülerden faydalınalarak nesne tabanlı sınıflandırma yöntemi ile kent merkezlerindeki detayların çıkarımı ve yorumlanması. Yüksek Lisans Tezi, Aksaray Üniversitesi, Fen Bilimleri Enstitüsü, Aksaray, 79.

Çömert R, Matcı D K, Avdan U (2017). Yıkılmış Binaların Nesne Tabanlı Sınıflandırma ile İnsansız Hava Aracı Verilerinden Tespit Edilmesi, 4. Uluslararası Deprem Mühendisliği ve Sismoloji Konferansı, Eskişehir.

Demir İ (2012). Hadoop tabanlı büyük ölçekli görüntü işleme altyapısı. Yüksek Lisans Tezi, Kocaeli Üniversitesi, Fen Bilimleri Enstitüsü, 87.

Demirci Ş, Özdemir C (2020). Anechoic Chamber Measurements for Circular Isar Imaging at Mersin University’s Meatr Lab. *IJEG*, 5 (3), 150-159.

Demirel A Ş (2010). Sayısal görüntü arşivi bilgi sistemi. Doktora tezi, Selçuk Üniversitesi, Fen Bilimleri Enstitüsü, 96.

DIN (1989). Regenwassernutzungsanlagen. Deutsches Institut Normung DIN: 1989, German.

Dorak S (2015). Nilüfer Çayı ve Nilüfer Çayı'na deşarj edilen kimi arıtma tesisi atık sularının sulama suyu kalite parametrelerinin belirlenmesi (Master's thesis, Uludağ Üniversitesi).

Eisfelder C, Kraus T, Bock M, Werner M, Buchroithner M F & Strunz G (2009). Towards automated forest-type mapping—a service within GSE Forest Monitoring based on SPOT-5 and IKONOS data. *International Journal of Remote Sensing*, 30(19), 5015-5038.

Erdoğan O (2002) Kocaeli İli Sahil Düzenlemesinin Sulama Sistemi Projelendirilmesi, Yüksek Lisans Tezi. İstanbul Üniversitesi Fen Bilimleri Enstitüsü Peyzaj Mimarlığı Ana Bilim Dalı, İstanbul, 55 s.

Eren B, Aygün A, Likos S & Damar A İ (2016). Yağmur Suyu Hasadı: Sakarya Üniversitesi Esentepe Kampüs Örneği. 4th International Symposium on Innovative Technologies in Engineering and Science 3-5November 2016 (ISITES2016 Alanya/Antalya - Turkey)

Fırat O & Erdoğan M (2015). Nesne (Obje) Tabanlı Sınıflandırma Tekniği İle Multispektral Hava Fotoğraflarından Otomatik Bina Çıkarımı, Tufuab VII. Teknik Sempozyumu 21-23 Mayıs 2015, Konya

Grigillo D & Kanjir U (2012). Urban object extraction from digital surface model and digital aerial images, *ISPRS Annals of the Photogrammetry, Remote Sensing and Spatial Information Sciences*, 3, 215-220, Melbourne, Australia

Hacar M (2020). A Rule-Based Approach for Generating Urban Footprint Maps: From Road Network to Urban Footprint. *IJEG*, 5 (2), 100-108.

- Haddeland I, Heinke J, Biemans H, Eisner S, Flörke M, Hanasaki N & Stacke T (2014). Global water resources affected by human interventions and climate change. *Proceedings of the National Academy of Sciences*, 111 (9), 3251-3256.
- Hoffman R & Jain A K (1987). Segmentation and classification of range images. *IEEE Transactions on Pattern Analysis and Machine Intelligence*, 9, 608-620.
- Paksoy teknik (2020a). http://www.paksoytekni.com.tr/images/paksoy-topcon/iha/parrot_bluegrass, [Access: 01.05.2020].
- Paksoy teknik (2020b). <http://www.paksoytekni.com.tr/images/PAKSOY-TOPCON/IHA/sensefly>, [Access: 01.05.2020].
- İncebel C (2012). Alternatif su kaynaklarının endüstriyel kullanıma kazandırılması için çatı yağmur suyu hasadı (Ostim örneği). Yüksek Lisans Tezi, Gazi Üniversitesi Fen Bilimleri Enstitüsü, Ankara.
- Kabadayı A & Uysal M (2020). Çok yüksek çözünürlüklü İHA verilerinden bina tespiti. *Türkiye İnsansız Hava Araçları Dergisi*, 2 (2), 43-48.
- Kalkan K & Maktav D (2010). Nesne Tabanlı Ve Piksel Tabanlı Sınıflandırma Yöntemlerinin Karşılaştırılması (İkonos Örneği), II. Uzaktan Algılama ve Coğrafi Bilgi Sistemleri Sempozyumu, 11 - 13, Gebze - KOCAELİ.
- Kantaroglu Ö (2009). Yağmur suyu hasadı plan ve hesaplama prensipleri. IX. Ulusal Tesi Mühendisliği Kongresi, 6-9 Mayıs, İzmir.
- Karlı F, Fidan M H & Dihkan M (2010). Kızılötesi Hava Fotoğraflarından Bina Detaylarının Çıkarılması. III. Uzaktan Algılama ve Coğrafi Bilgi Sistemleri Sempozyumu, 11-13, Gebze - KOCAELİ.
- Kavzoğlu T & Çölkesen İ (2010). Destek vektör makineleri ile uydu görüntülerinin sınıflandırılmasında kernel fonksiyonlarının etkilerinin incelenmesi. *Harita Dergisi*, 144 (7), 73-82.
- Kaya Y (2020). Çok bantlı uydu görüntüleri kullanılarak buğday bitkisinin incelenmesi - Ceylanpınar TİGEM örneği. Yüksek Lisans Tezi, Harran Üniversitesi, Fen Bilimleri Enstitüsü, 84.
- Kılıç M Y & Abuş M N (2018). Bahçeli Bir Konut Örneğinde Yağmur Suyu Hasadı. *Uluslararası Tarım ve Yaban Hayatı Bilimleri Dergisi*, 4(2), 209-215.
- Kılıç S (2008). Küresel İklim Değişikliği Sürecinde Su Yönetimi. İ.Ü. Siyasal Bilgiler Fakültesi Dergisi, 39, 161-186.
- Kraus K (2011). *Photogrammetry: geometry from images and laser scans*. Walter de Gruyter.
- Lu D, Mausel P, Brondizio E & Moran E (2004). Change detection techniques. *INT. J. REMOTE SENSING*, 25 (12), 2365-2407.
- Marangoz A M (2009). Uydu görüntülerinden kentsel ayrıntıların nesne-tabanlı sınıflandırma yöntemiyle belirlenmesi ve cbs ortamında bütünleştirilmesi, Doktora tezi, Yıldız Teknik Üniversitesi, Fen Bilimleri Enstitüsü, İstanbul, 133.
- Motohka T, Nasahara K N, Oguma H & Tsuchida S (2010). Applicability of green-red vegetation index for remote sensing of vegetation phenology. *Remote Sensing*, 2, 2369-2387.
- Olaniyi O A, Olutimehin I.O & Funmilayo O A (2019). Review of climate change and its effect on Nigeria ecosystem. *International journal of Rural Development, Environment and Health Research*, 3 (3).
- Orhan O & Yakar M (2016). Investigating land surface temperature changes using Landsat data in Konya, Turkey. *International Archives of Photogrammetry, Remote Sensing and Spatial Information Sciences*, 41, 285-89.
- Oweis T & Prinz Dand Hachum A (2001). Water Harvesting: Indigenous Knowledge for The Future of The Drier Environments. International Center for Agricultural Research in the Dry Areas (ICARDA), Aleppo, Syria.
- Rouse Jr J W, Haas R H, Deering D W, Schell J A & Harlan J C (1974). Monitoring the Vernal Advancement and Retrogradation (Green Wave Effect) of Natural Vegetation.
- Şahin N & Manioğlu G (2011). Binalarda yağmur suyunun kullanılması. *Tesi Mühendisliği*, 125: 21-32.
- Sandalcı M & Yüksel İ (2011). İklim Değişikliğinin Türkiye'deki Göller ve Barajlar Üzerindeki Etkisi, *Yapı Dünyası Dergisi*, 181, 25 - 29, 2011.
- Saritur B, Bayram B, Duran Z, Seker D (2020). Feature Extraction from Satellite Images Using Segnet and Fully Convolutional Networks (FCN). *International Journal of Engineering and Geosciences*, 5 (3), 138-143.
- Şasi A & Yakar M (2018). Photogrammetric modelling of hasbey dar'ülhuffaz (masjid) using an unmanned aerial vehicle. *International Journal of Engineering and Geosciences*, 3 (1), 6-11.
- SFR (2017). Yağmur suyu filtreleme ve depolama sistemi. <http://www.sfr.com.tr/yagmur-suyu-hasati-s6.html> [Access: 08.11.2020].
- Sonnentag O, Hufkens K, Teshera-Sterne C, Young A M, Friedl M, Braswell B H & Richardson A D (2012). Digital repeat photography for phenological research in forest ecosystems. *Agricultural and Forest Meteorology*, 152, 159-177.
- Sturm M, Zimmermann M, Schutz K, Urban W & Hartung H (2009). Rainwater harvesting as an alternative Water resource in rural sites in central northern Namibia. *Physics and Chemistry of the Earth*, 34: 776-785.
- Tanık A (2017). Yağmur Suyu Toplama, Biriktirme ve Geri Kullanımı (Doctoral dissertation, Yüksek Lisans Tezi, İTÜ İnşaat Fakültesi, Çevre Mühendisliği Bölümü).
- Tema (2020). TEMA-Geleceğin suyu. http://sutema.org/resources/Document/FileName/2015-12-01_22-11-14-692%20GeleceginSuyu.pdf [Access: 15.11.2020].

Tıkansak T E (2013). Konutlarda enerji etkinliği. <https://www.tse.org.tr/Icerik/HaberDetay?HaberID=13010> [Access: 19.11.2020].

Trenberth K E (2011). Changes in precipitation with climate change. *Climate Research*, 47 (1-2), 123-138.

Ulusoy K (2007), Küresel Ticaretin Son Hedefi: Su Pazarı, Kristal Kitaplar Yayınevi,

Ulvi A, Yakar M, Yiğit A Y & Kaya Y (2020). İHA ve Yersel Fotogrametrik Teknikler Kullanarak Aksaray Kızıl Kilise'nin 3 Boyutlu Nokta Bulutu ve Modelinin Üretilmesi. *Geomatik Dergisi*, 5 (1), 22-30.

Utsav R P, Vikrant A P, Manjurali I B & Harhad M R (2014). Rooftop Rainwater Harvesting (RRWH) at SPSV Campus, Visnagar: Gujarat - A Case Study.

IJRET: International Journal of Research in Engineering and Technology, 3 (4), 821-825

Yiğit A Y & Kaya Y (2020). Sentinel-2A uydu verileri kullanılarak sel alanlarının incelenmesi: Düzce örneği. *Türkiye Uzaktan Algılama Dergisi*, 2(1), 1-9.

Yiğit A Y & Uysal M (2019a). Nesne tabanlı sınıflandırma yaklaşımı kullanılarak yolların tespiti. *Türkiye Fotogrametri Dergisi*, 1 (1), 17-24.

Yiğit A Y & Uysal M (2019b). Nesne Tabanlı Sınıflandırma ile Taşkın Alanlarının Analizi. *Resilience*, 3(2), 369-385.

Yiğit A Y & Uysal M (2020). Automatic road detection from orthophoto images. *Mersin Photogrammetry Journal*, 2 (1), 10-17.



© Author(s) 2020. This work is distributed under <https://creativecommons.org/licenses/by-sa/4.0/>